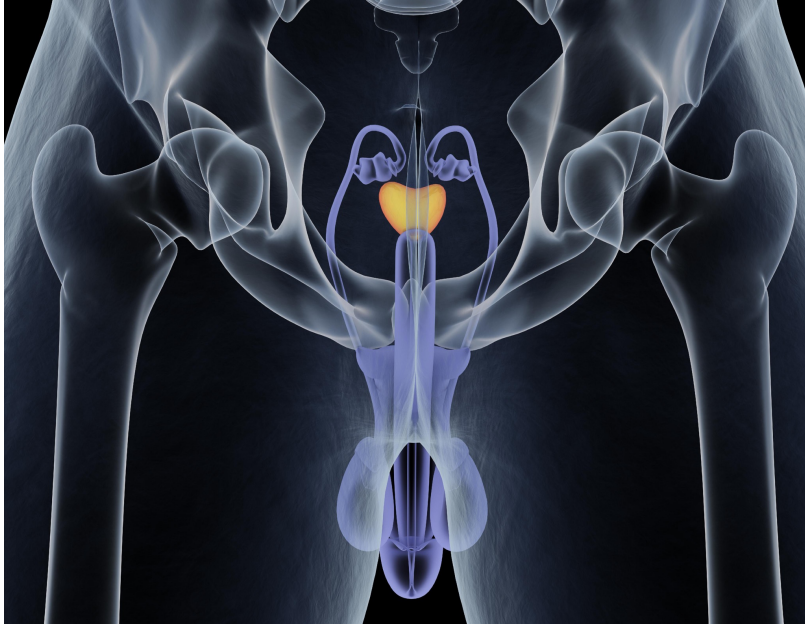


L6 – KB-0742: A Phase 2 clinical candidate discovered by SMMs

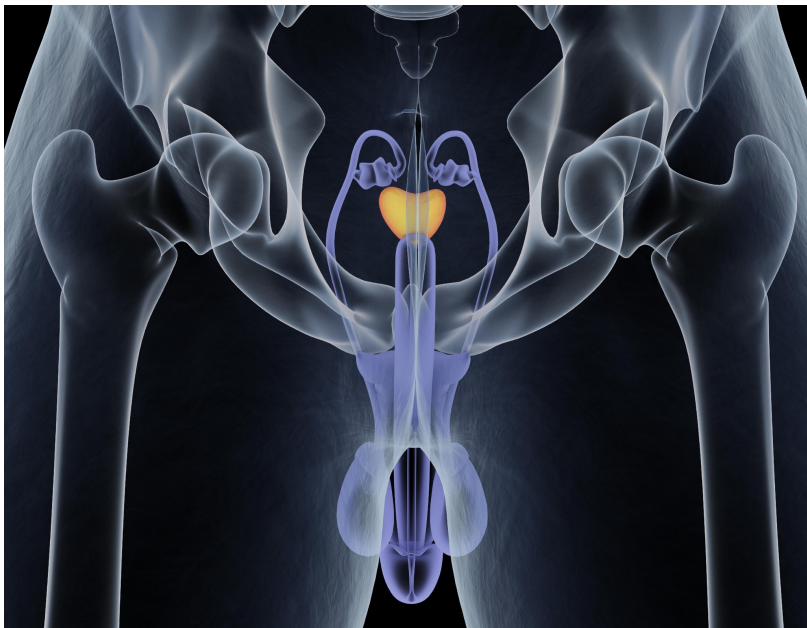
March 2nd, 2023

Prostate Cancer



Other than skin cancer, prostate cancer is the most common cancer in men

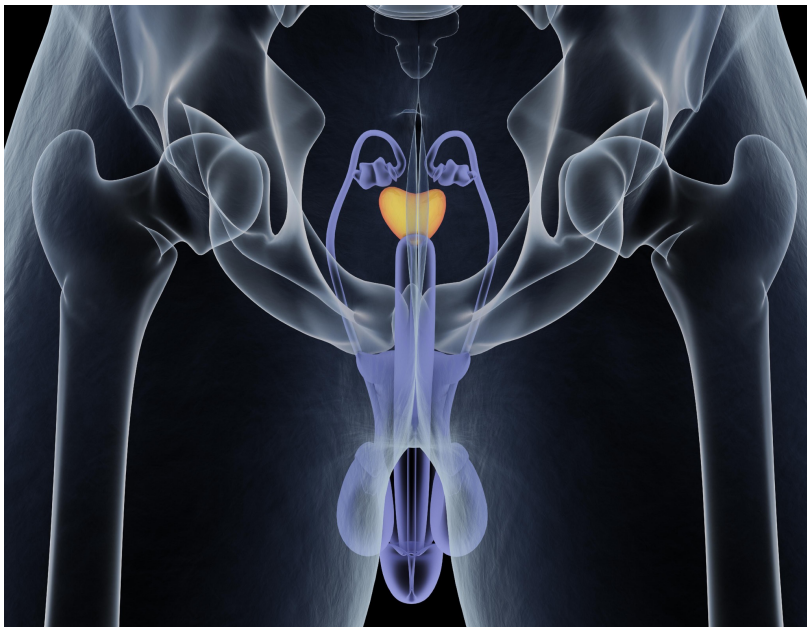
Prostate Cancer



Other than skin cancer, prostate cancer is the most common cancer in men

2023 US estimates: 288,300 new cases
 34,700 deaths

Prostate Cancer

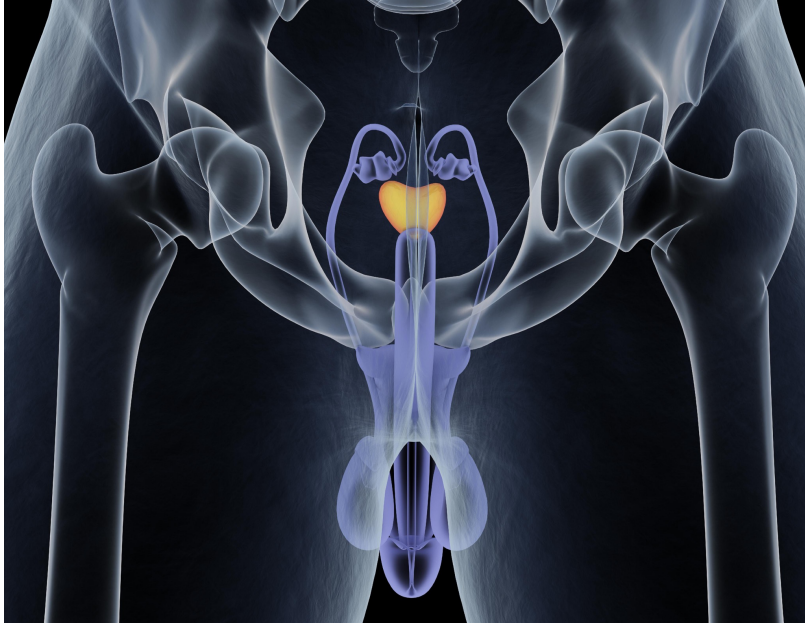


Other than skin cancer, prostate cancer is the most common cancer in men

2023 US estimates: 288,300 new cases
 34,700 deaths

1 out of 8 men will be diagnosed in their lifetime

Prostate Cancer



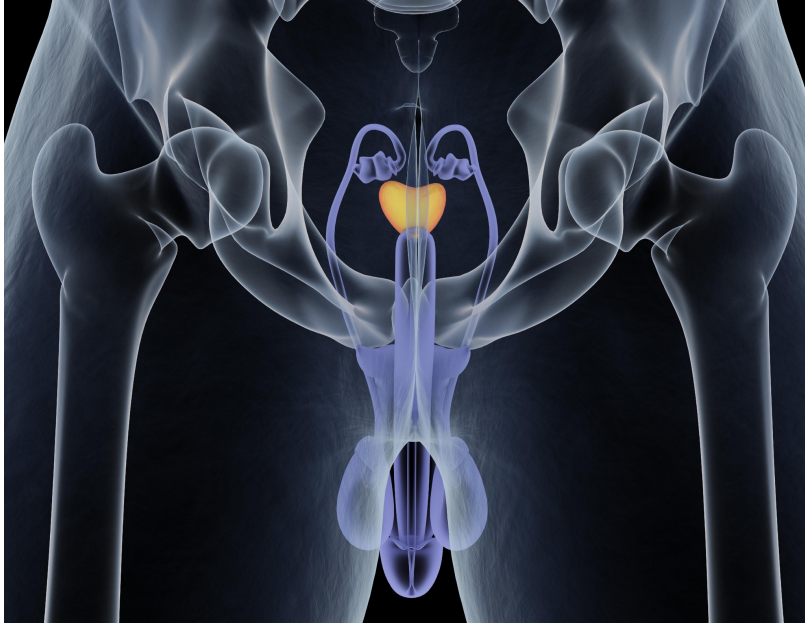
Other than skin cancer, prostate cancer is the most common cancer in men

2023 US estimates: 288,300 new cases
 34,700 deaths

1 out of 8 men will be diagnosed in their lifetime

Develops more frequently in older men (6 out of 10 cases in men 65-yo or older), rare under 40-yo

Prostate Cancer



Other than skin cancer, prostate cancer is the most common cancer in men

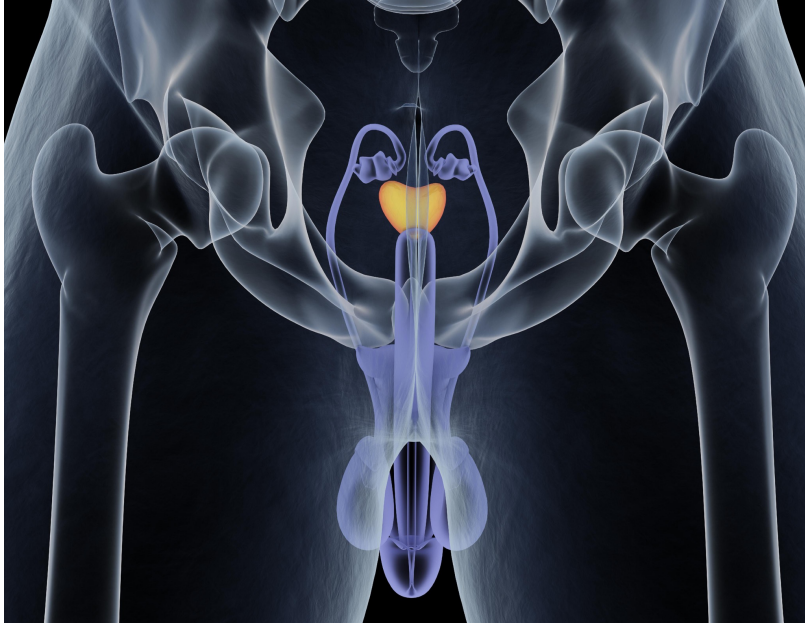
2023 US estimates: 288,300 new cases
 34,700 deaths

1 out of 8 men will be diagnosed in their lifetime

Develops more frequently in older men (6 out of 10 cases in men 65-yo or older), rare under 40-yo

Avg. age of first diagnosis is 66-yo

Prostate Cancer



Other than skin cancer, prostate cancer is the most common cancer in men

2023 US estimates: 288,300 new cases
 34,700 deaths

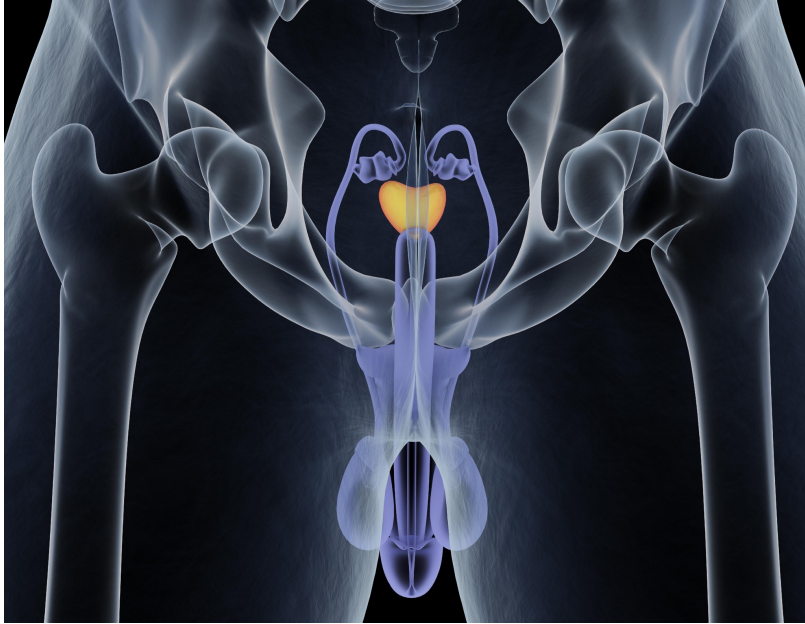
1 out of 8 men will be diagnosed in their lifetime

Develops more frequently in older men (6 out of 10 cases in men 65-yo or older), rare under 40-yo

Avg. age of first diagnosis is 66-yo

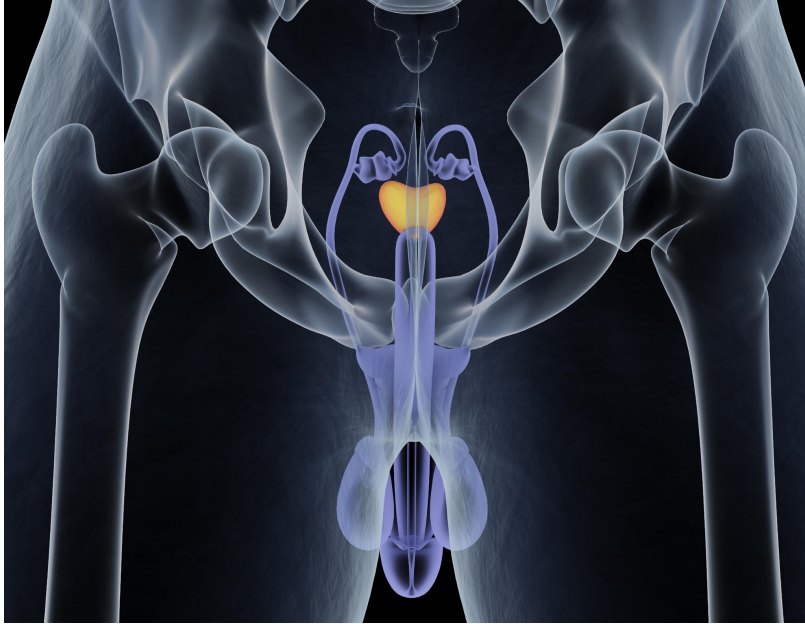
More common in non-Hispanic Black men:
1.7x diagnoses
2.1x deaths

Prostate Cancer



Second-leading cause of death in American men,
behind only lung cancer

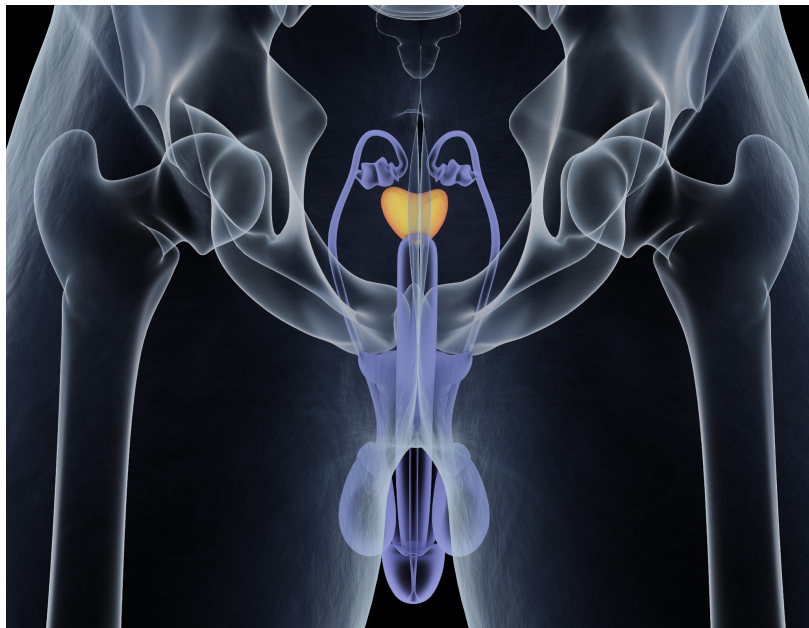
Prostate Cancer



Second-leading cause of death in American men,
behind only lung cancer

1 out of 41 men will die of prostate cancer

Prostate Cancer

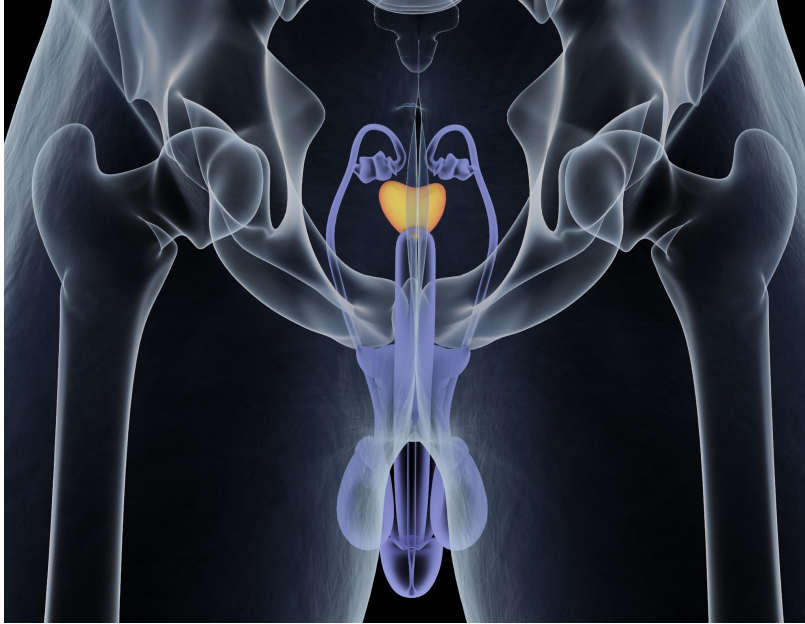


Second-leading cause of death in American men, behind only lung cancer

1 out of 41 men will die of prostate cancer

Most men survive and do not die from this cancer.
>3.1 million diagnosed men in the US are alive today

Prostate Cancer



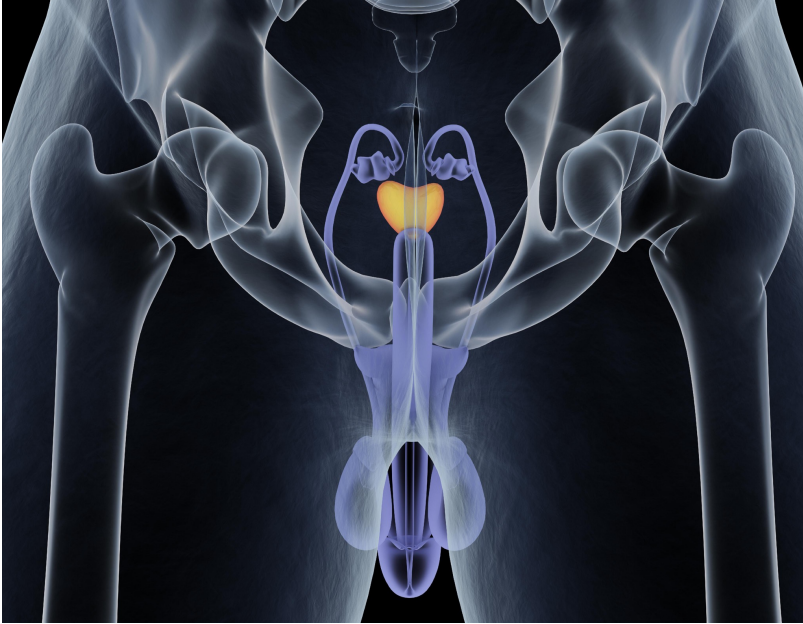
Second-leading cause of death in American men, behind only lung cancer

1 out of 41 men will die of prostate cancer

Most men survive and do not die from this cancer.
>3.1 million diagnosed men in the US are alive today

1993-2013: death rate declined by half, likely due to earlier detection and advances in treatment

Prostate Cancer



Second-leading cause of death in American men, behind only lung cancer

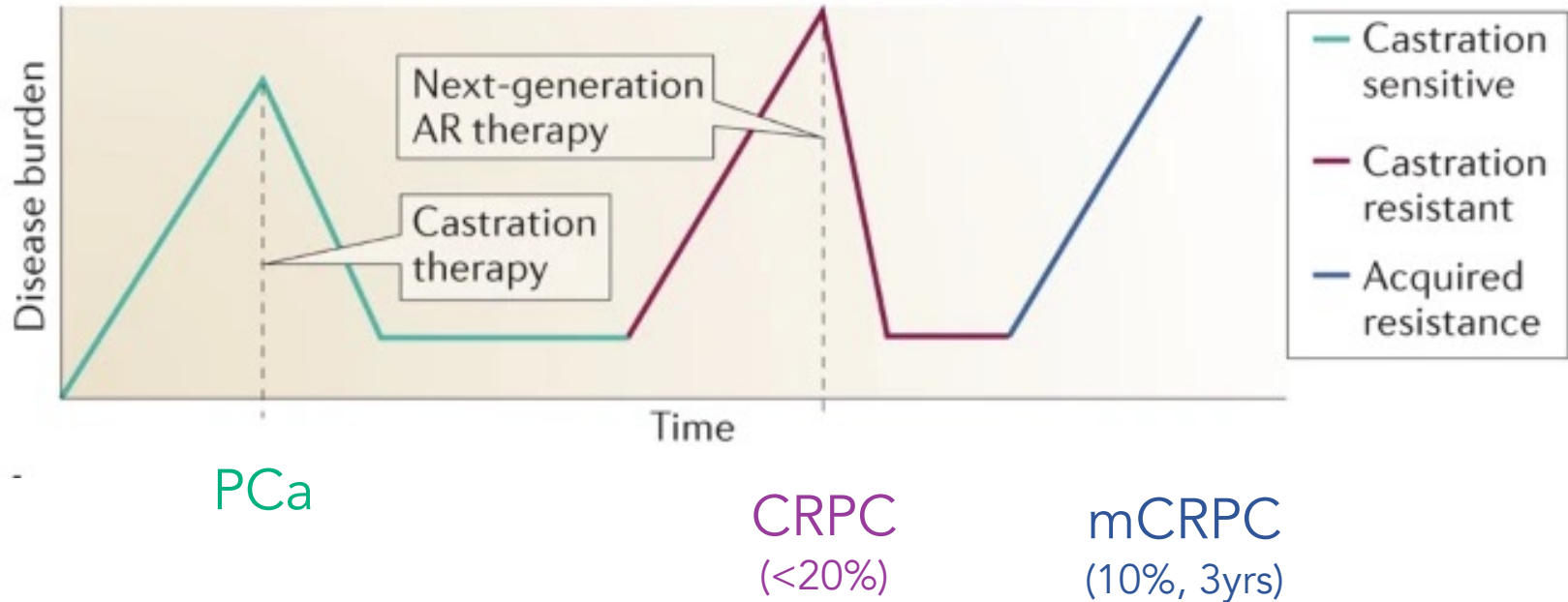
1 out of 41 men will die of prostate cancer

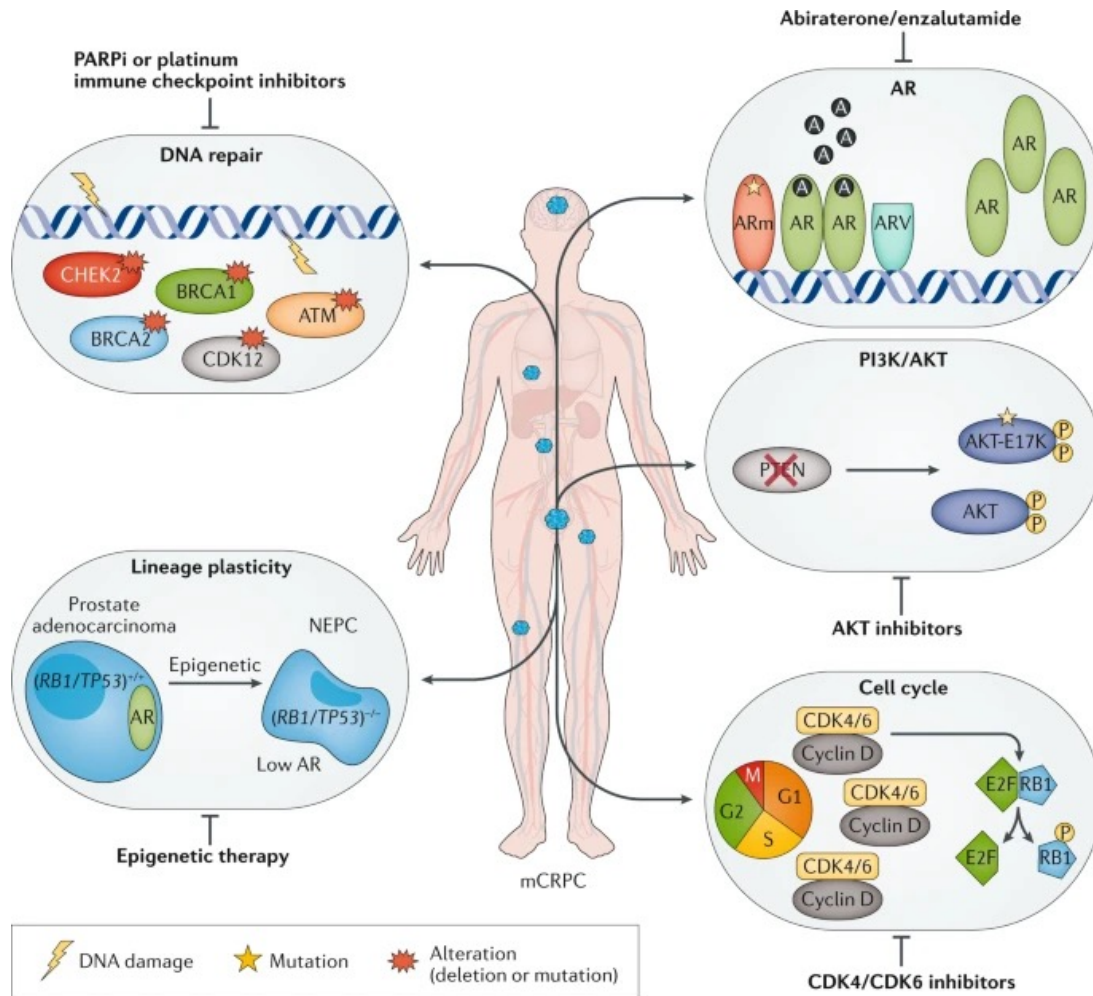
Most men survive and do not die from this cancer.
>3.1 million diagnosed men in the US are alive today

1993-2013: death rate declined by half, likely due to earlier detection and advances in treatment

2013 onward: pace of decline slowed, likely reflecting the rise in cancers found at an **advanced stage with resistance to therapies**

Increasing disease burden following primary prostate cancer therapy

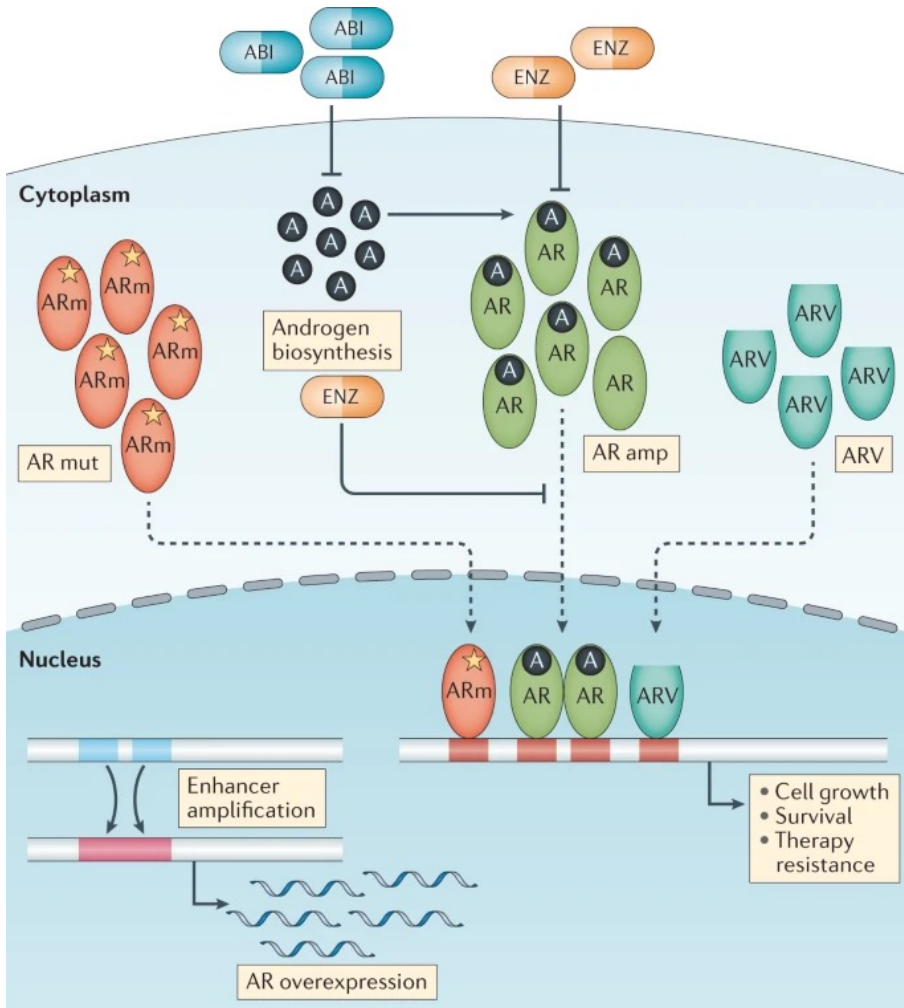




Molecular landscape of advanced disease

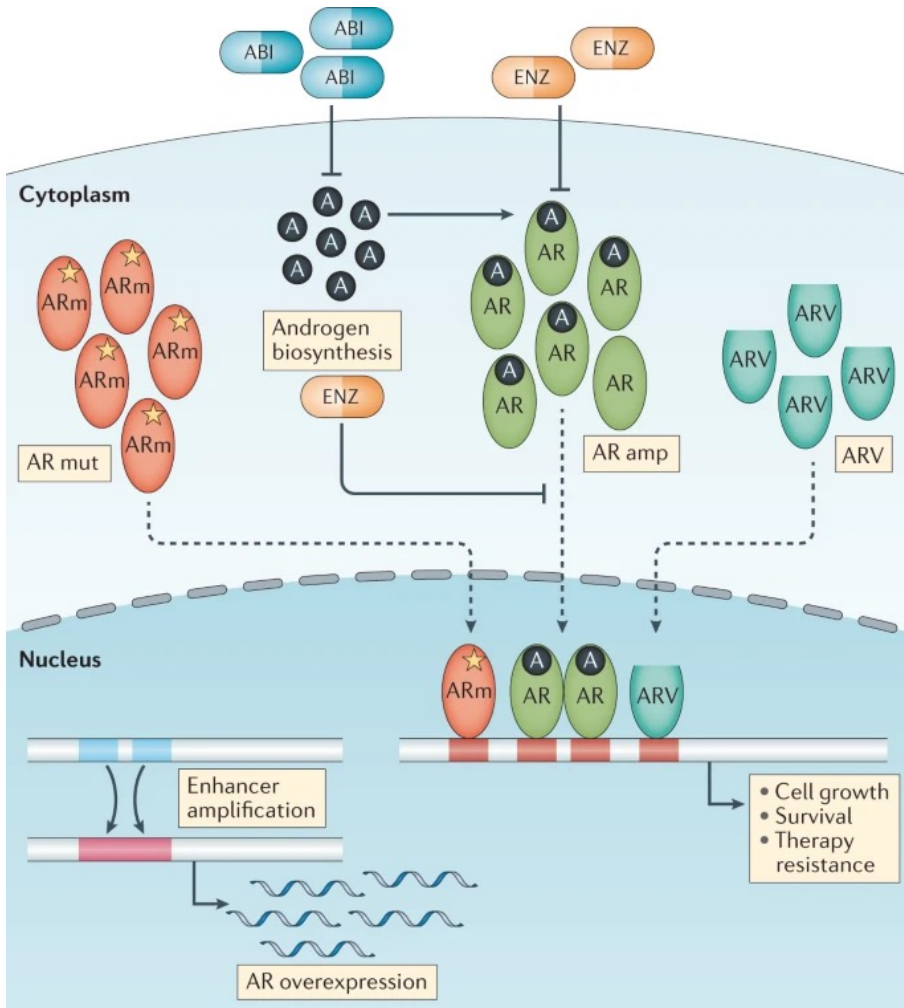
Genomic alterations are heterogenous across patients with metastatic castration-resistant prostate cancer (mCRPC)

By understanding the genes or pathways altered in any given individual, precision medicine has the potential to improve clinical outcomes.



Alterations in Androgen Receptor (AR) signaling are the most prevalent events in metastatic castration-resistant prostate cancer leading to *persistent AR activation*

- AR amplifications (AR amp)
- AR mutations (AR mut)
- AR splice variants (ARVs)
- Intratumoral androgen biosynthesis
- AR enhancer amplification



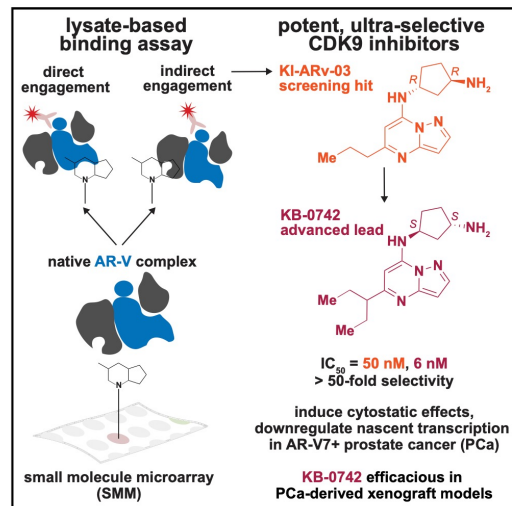
Alterations in Androgen Receptor (AR) signaling are the most prevalent events in metastatic castration-resistant prostate cancer leading to *persistent AR activation*

- AR amplifications (AR amp)
- AR mutations (AR mut)
- AR splice variants (ARVs)**
- Intratumoral androgen biosynthesis
- AR enhancer amplification

Cell Chemical Biology

Modulating Androgen Receptor-Driven Transcription in Prostate Cancer with Selective CDK9 Inhibitors

Graphical Abstract



Highlights

- KI-ARv-03 reduces AR protein levels and AR-driven transcription
- KI-ARv-03 is deduced to be a potent, ultrasensitive inhibitor of CDK9
- Optimization led to the orally bioavailable and selective CDK9 inhibitor KB-0742
- KB-0742 displays potent anti-tumor activity in cancer models *in vitro* and *in vivo*

Authors

André Richters, Shelby K. Doyle, David B. Freeman, ..., Charles Y. Lin, Marius S. Pop, Angela N. Koehler

Correspondence

koehler@mit.edu

In Brief

In the pursuit of hormone receptor modulators in prostate cancer, a potent, ultrasensitive CDK9 inhibitor is discovered. This study describes the most selective inhibitors of CDK9 known to date and provides compelling preclinical *in vitro* and *in vivo* support for CDK9 as a therapeutic target.



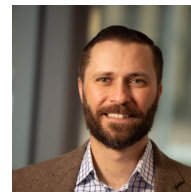
André Richters



Shelby Doyle



Becky Leifer



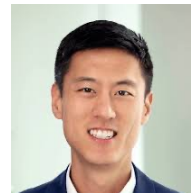
David Freeman



Marius Pop



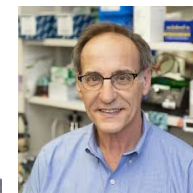
Nick Struntz



Charles Lin



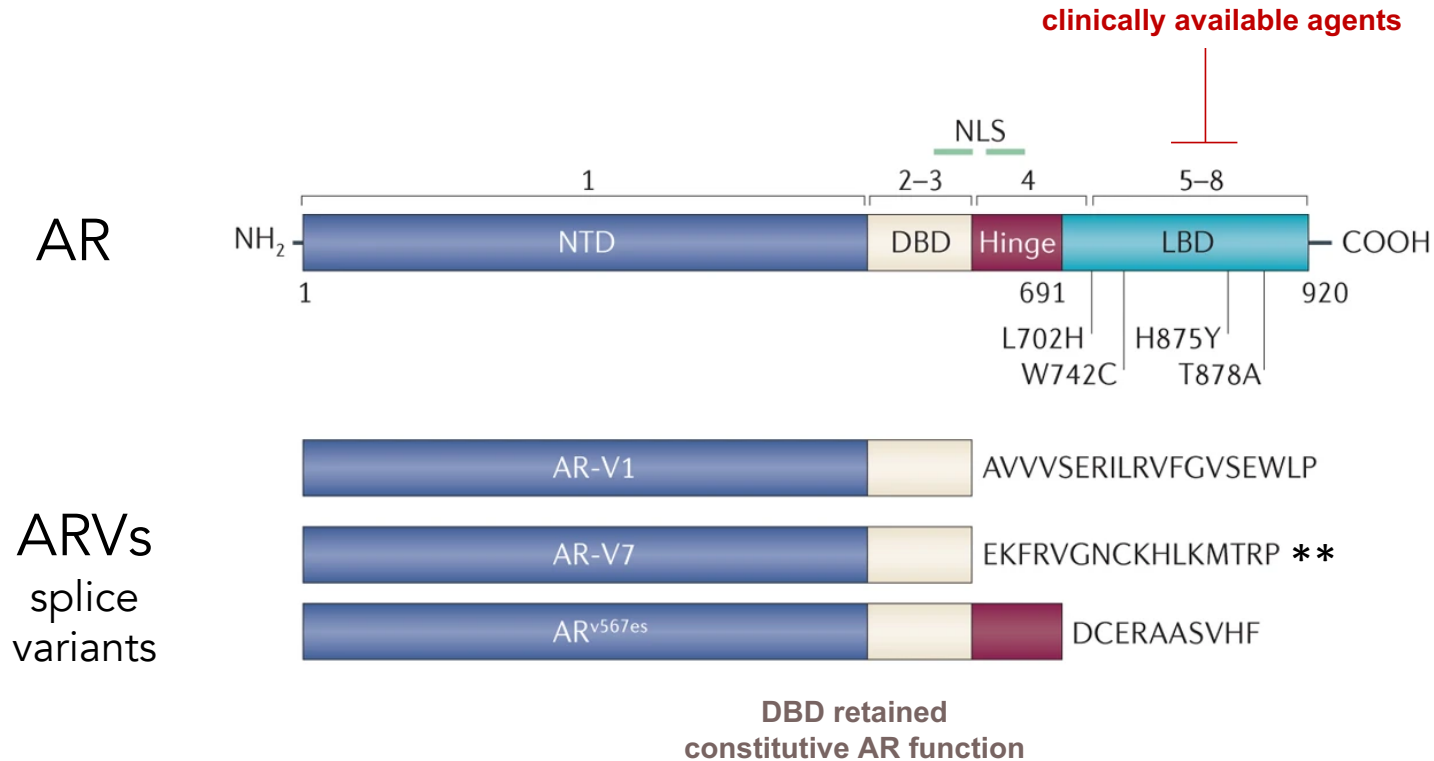
Stefan Knapp



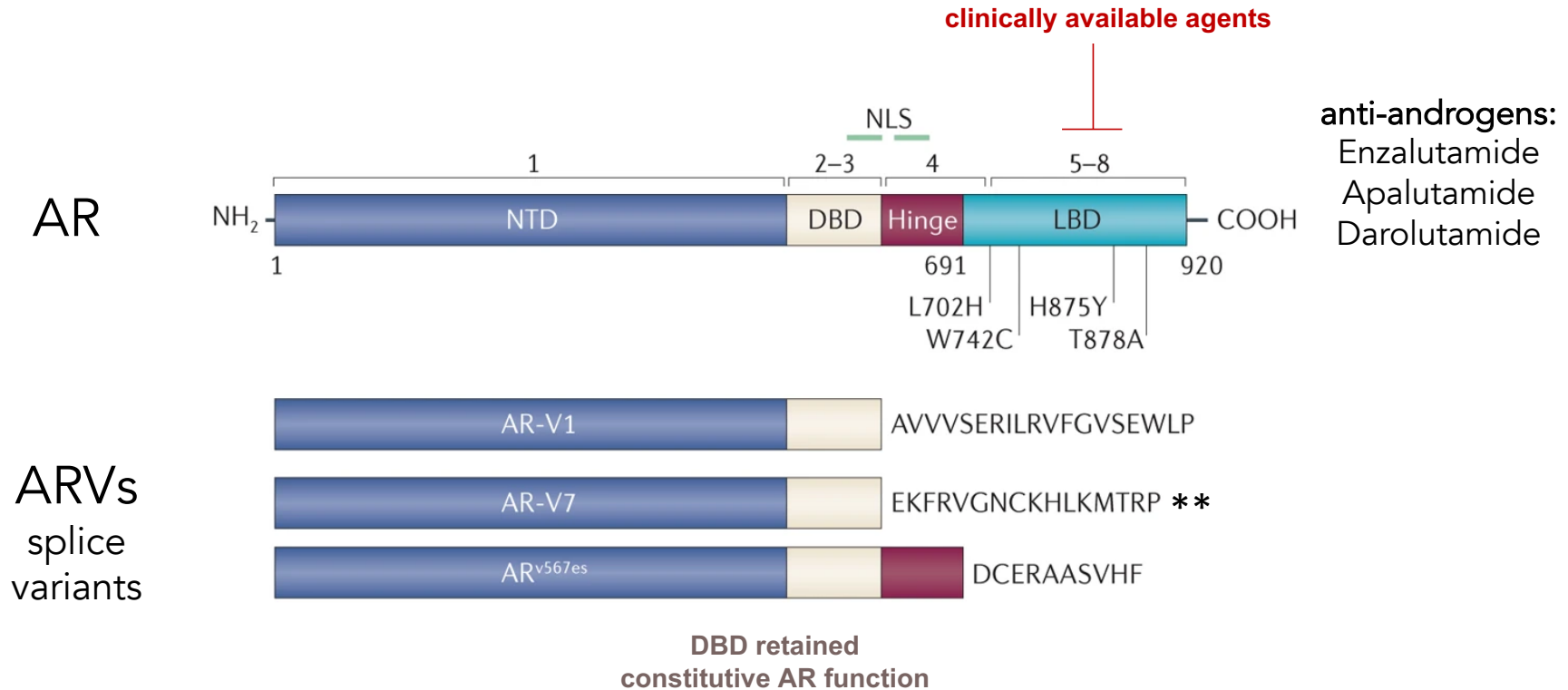
Steven Balk



Domain structure of AR, cancer-associated mutations, and splice variants

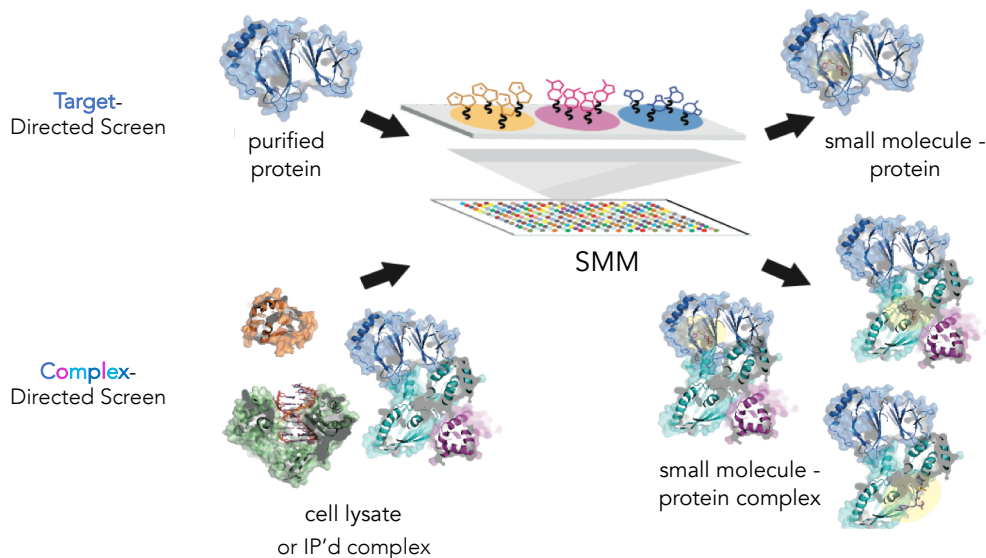


Domain structure of AR, cancer-associated mutations, and splice variants

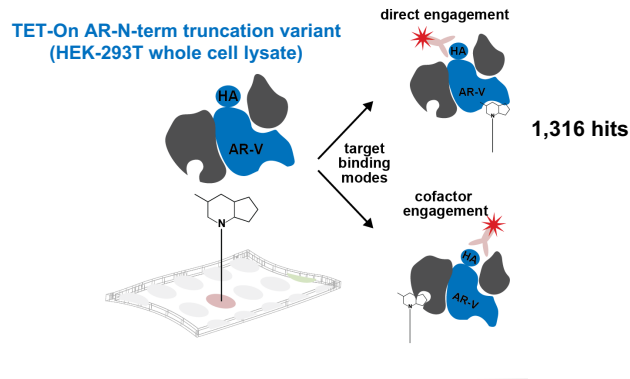


Rationale:

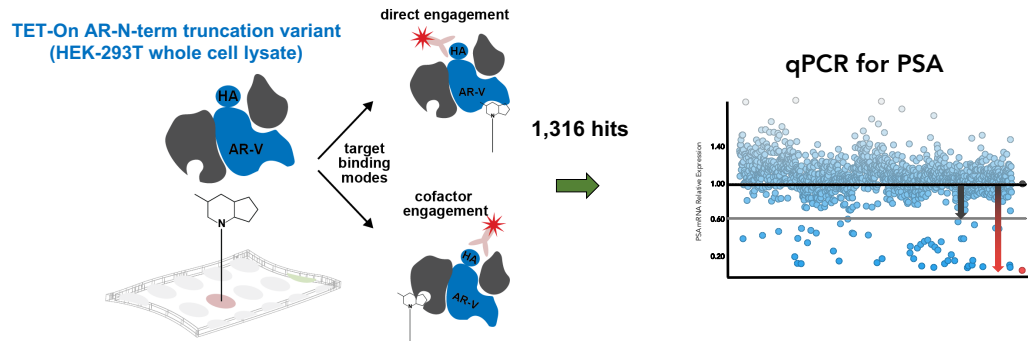
- (1) AR splice variants lack ligand binding domain (LBD), contributing to resistance associated with AR antagonists in CRPC,
- (2) screening ARv-containing complexes in cell lysates avoids purification,
- (3) reflects more relevant state, and casts a net for targeting co-factors.



Active compounds prioritized in prostate-specific antigen (PSA) expression and AR reporter assays

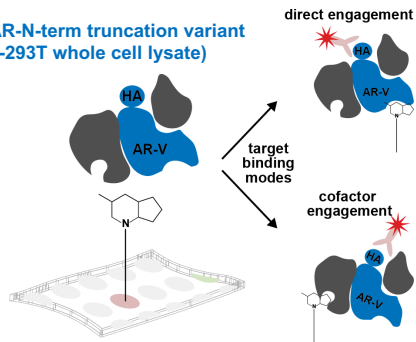


Active compounds prioritized in prostate-specific antigen (PSA) expression and AR reporter assays

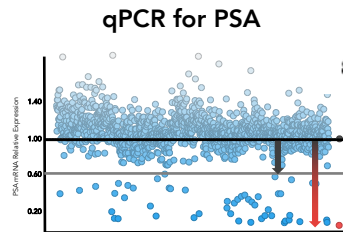


Active compounds prioritized in prostate-specific antigen (PSA) expression and AR reporter assays

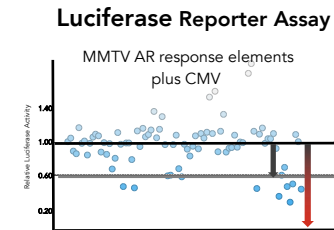
TET-On AR-N-term truncation variant
(HEK-293T whole cell lysate)



1,316 hits



85 compounds

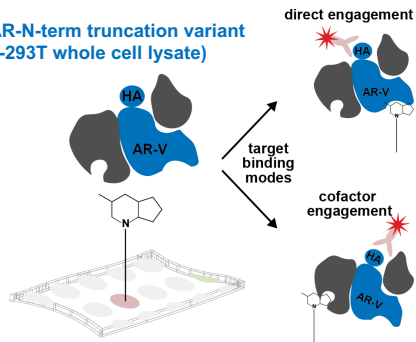


7 reasonable actives, 3 prioritized



Active compounds prioritized in prostate-specific antigen (PSA) expression and AR reporter assays

TET-On AR-N-term truncation variant
(HEK-293T whole cell lysate)

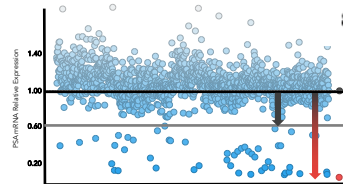


direct engagement



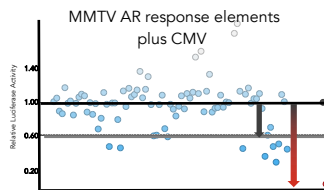
1,316 hits

qPCR for PSA

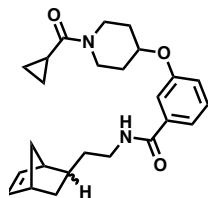


85 compounds

Luciferase Reporter Assay



7 reasonable actives, 3 prioritized

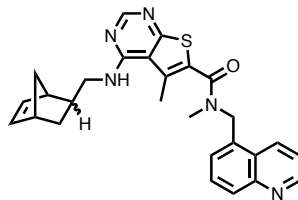


KI-ARv-01

MW = 408.54

cLogP = 3.27

IC₅₀ = 5.43 μM

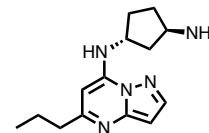


KI-ARv-02

MW = 469.61

cLogP = 5.48

IC₅₀ = 6.86 μM



KI-ARv-03

MW = 259.36

cLogP = 2.55

IC₅₀ = 7.61 μM

KI-ARv-03 impacts AR-V7 levels in an enzalutamide-resistant prostate cancer cellular model



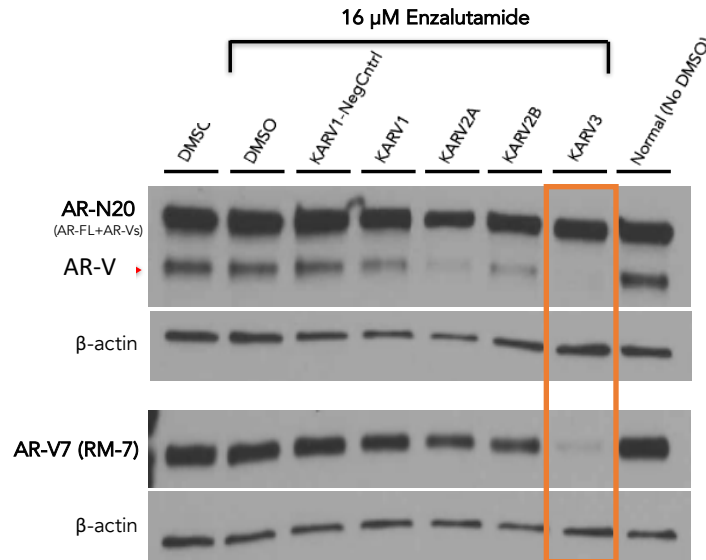
Dr. Joshua Russo



Dr. Steven Balk

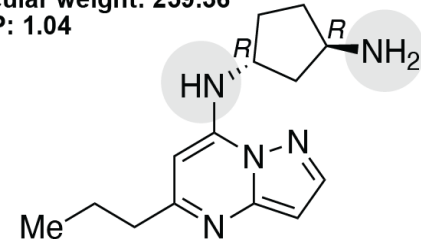
VCaP-16 cells

enzalutamide-resistant
increased expression of AR-v7
5 μM compound, 24-hour exposure



KI-ARv-03

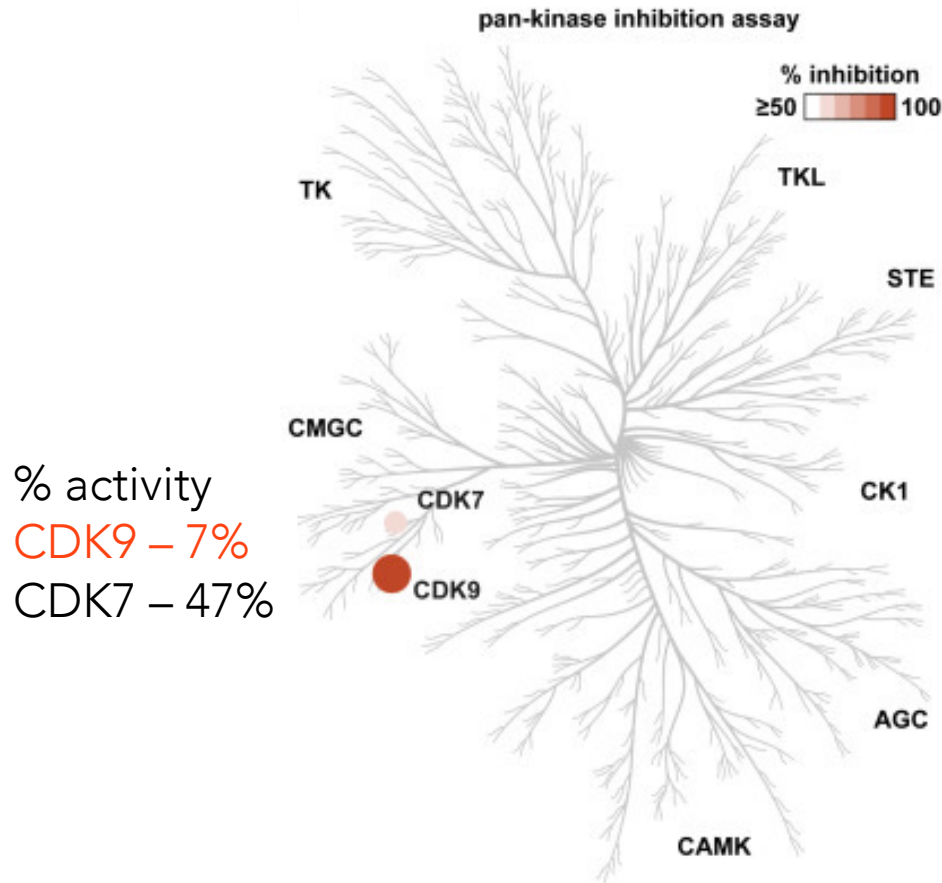
molecular weight: 259.36
cLogP: 1.04



assay	cell line	IC ₅₀ (μM)	
ARv driven PSA reporter 24h	LNCaP	7.6	mutAR+
Cell viability cell-titer glo 72h	LNCaP	7.7	mutAR+
	VCaP	7.9	AR+
	DU145	9.3	AR-
	PC3	17	AR-

nM inhibitor in MYC-driven reporter assay?

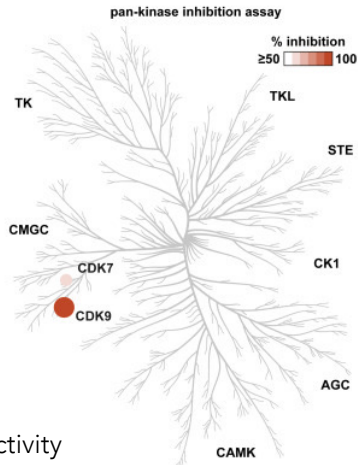
Kinase selectivity profiling suggests CDK9 as a target



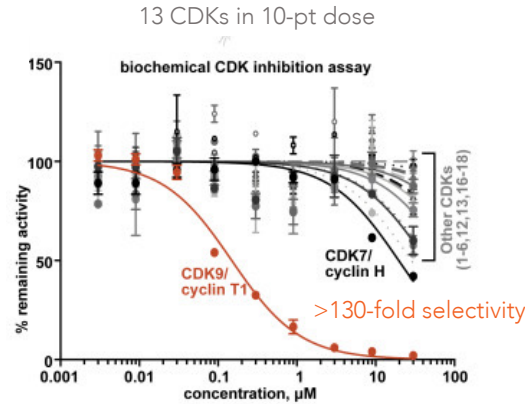
10 μ M KI-ARv-03
[ATP] -/+ 15 μ M
apparent K_m
for each kinase

Kinase selectivity profiling suggests CDK9 as a target

10 μM KI-ARV-03
[ATP] +/- 15 μM
apparent K_m
for each kinase



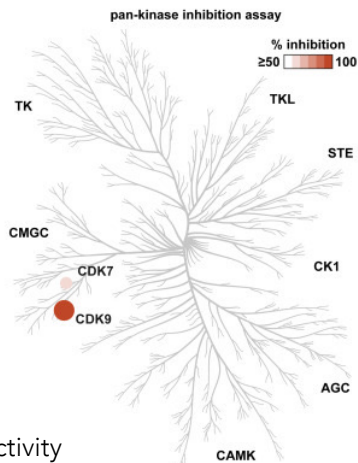
% activity
CDK9 – 7%
CDK7 – 47%



CDK9 IC_{50} = 0.15 μM (45 μM ATP)
CDK7 IC_{50} = 20.1 μM

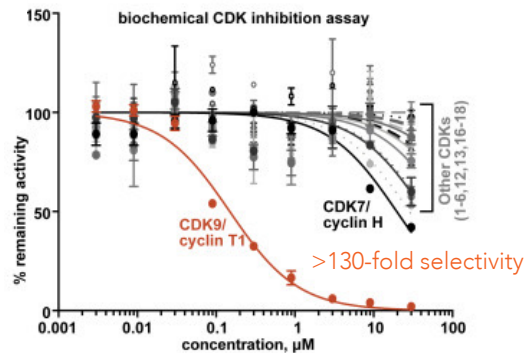
Kinase selectivity profiling suggests CDK9 as a target

10 μM KI-ARV-03
[ATP] +/- 15 μM
apparent K_m
for each kinase



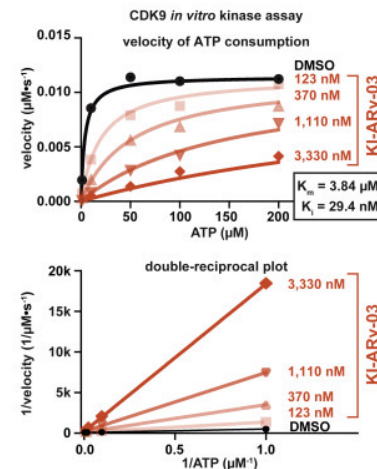
% activity
CDK9 – 7%
CDK7 – 47%

13 CDKs in 10-pt dose



CDK9 IC_{50} = 0.15 μM (45 μM ATP)
CDK7 IC_{50} = 20.1 μM

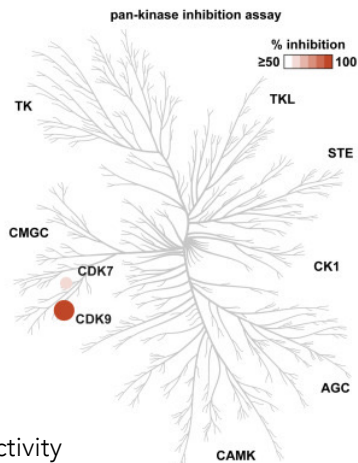
Michaelis-Menten and Lineweaver-Burk



ATP
competitive

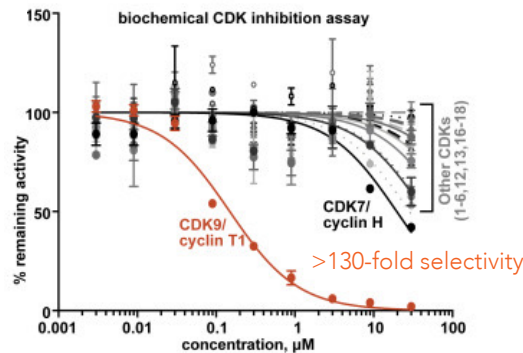
Kinase selectivity profiling suggests CDK9 as a target

10 μM KI-ARv-03
[ATP] +/- 15 μM
apparent K_m
for each kinase



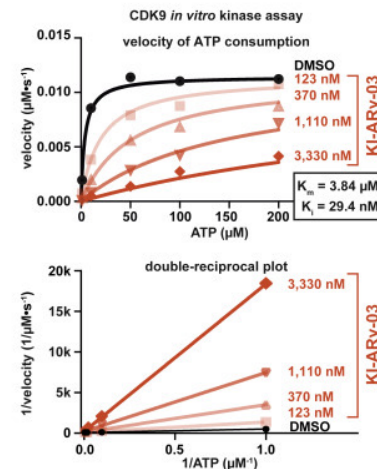
% activity
CDK9 – 7%
CDK7 – 47%

13 CDKs in 10-pt dose



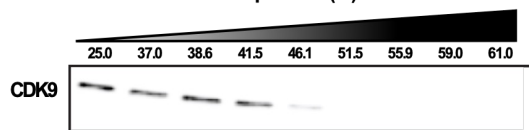
CDK9 IC_{50} = 0.15 μM (45 μM ATP)
CDK7 IC_{50} = 20.1 μM

Michaelis-Menten and Lineweaver-Burk

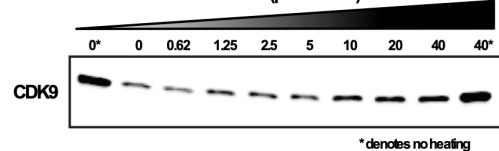


ATP
competitive

CETSA melt curve
temperature ($^{\circ}\text{C}$)



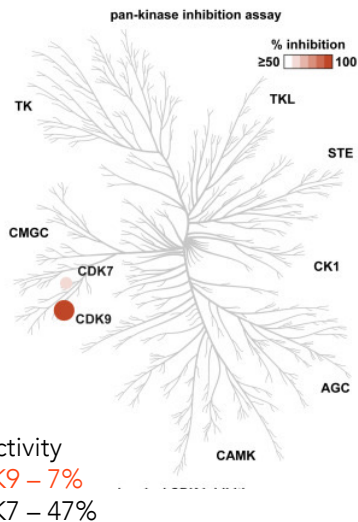
isothermal dose finger print
KI-ARv-03 (μM at 49°C)



stabilization in live 22RV1 cells

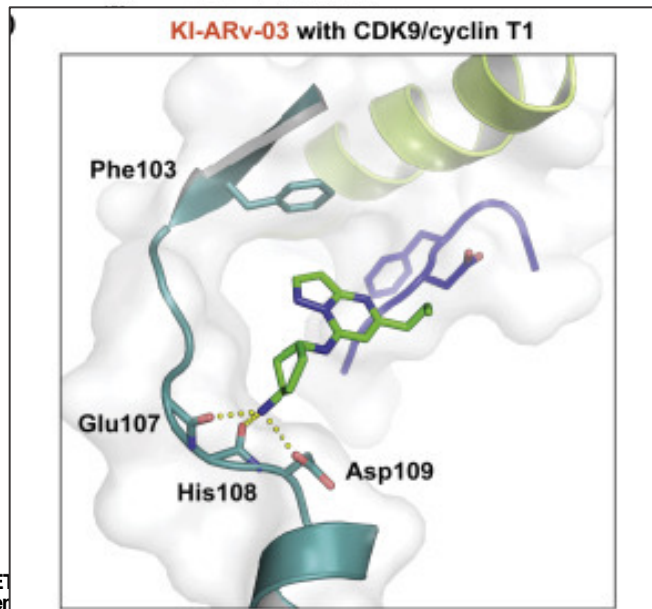
Kinase selectivity profiling suggests CDK9 as a target

10 μM KI-ARv-03
[ATP] \pm 15 μM
apparent K_m
for each kinase

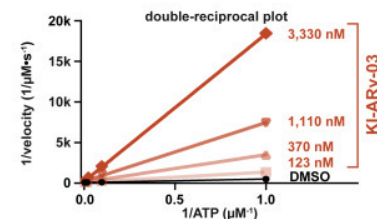
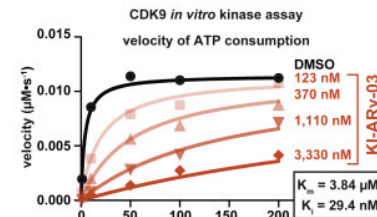


% activity
CDK9 – 7%
CDK7 – 47%

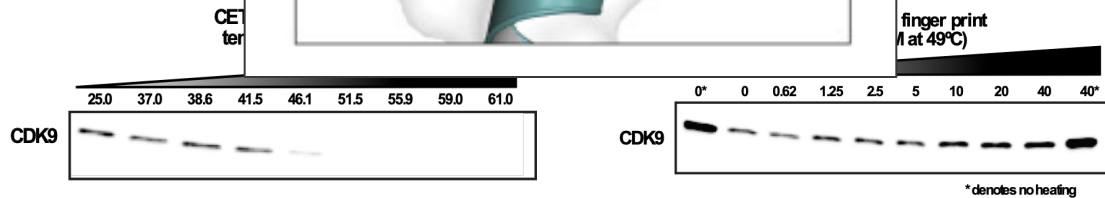
13 CDKs in 10-pt dose



Michaelis-Menten and Lineweaver-Burk



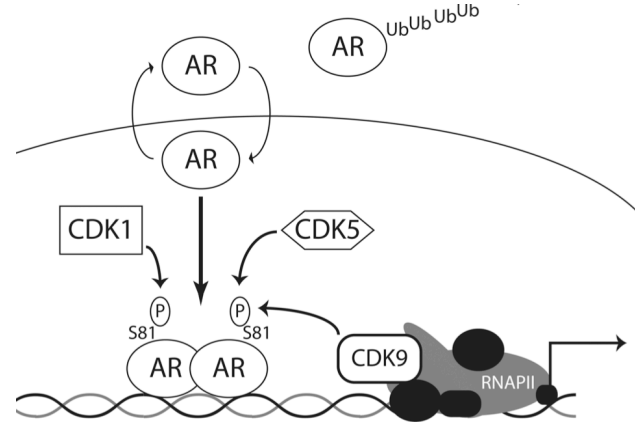
ATP
competitive



stabilization in live 22RV1 cells

CDK9 is a known regulator of AR/ARV species activity

CDK9 regulates AR and ARV activity, stability through N-terminal S81

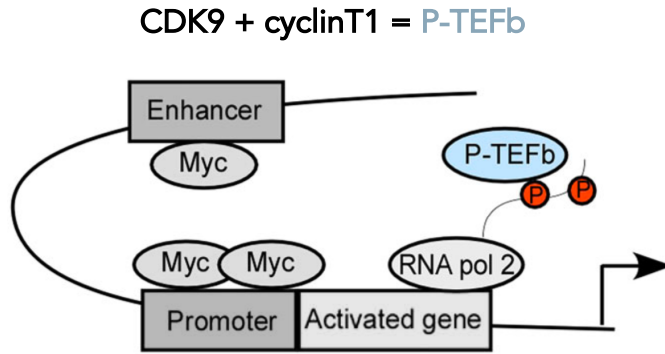


Koryakina, Y., Ta, H. Q., and Gioeli, D. (2014) *Endocr. Relat. Cancer* 21, T131–45.

ARVs (and AR) physically interact with CDK9 in cells

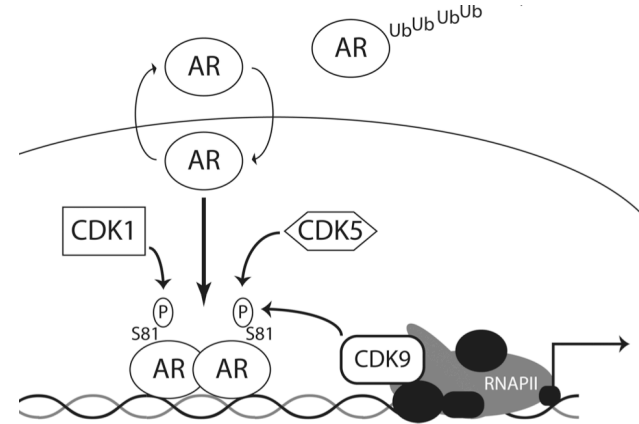
CDK9 is a known regulator of AR/ARV species activity

transcriptional oncogene activity frequently
reliant on CDK9 via elongation factor P-TEFb



Chen, H., Liu, H., and Qing, G. (2018) *Sig Transduct Target Ther* 3, 635–7
Bai et al., (2019) *Oncogene* 38, 4977-4989
Huang et al. (2014) *Genes Dev* 28, 1800-1814

CDK9 regulates AR and ARV
activity, stability through N-terminal S81

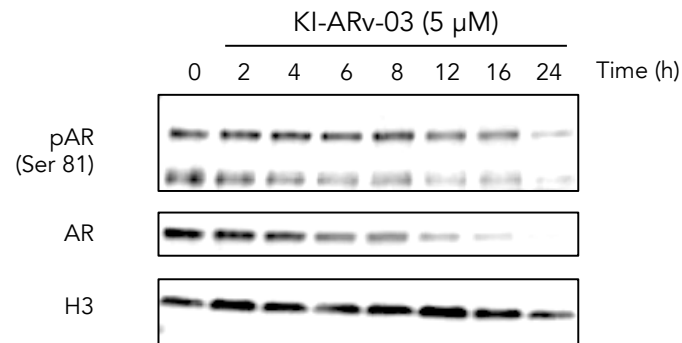
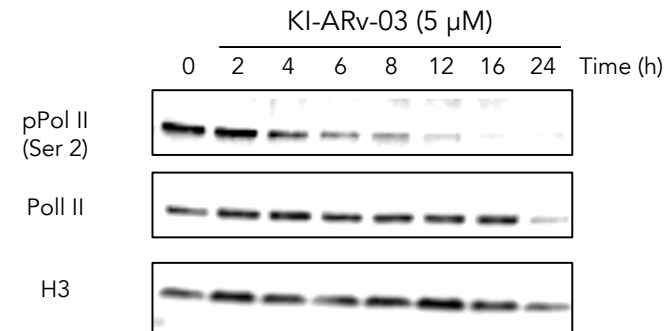
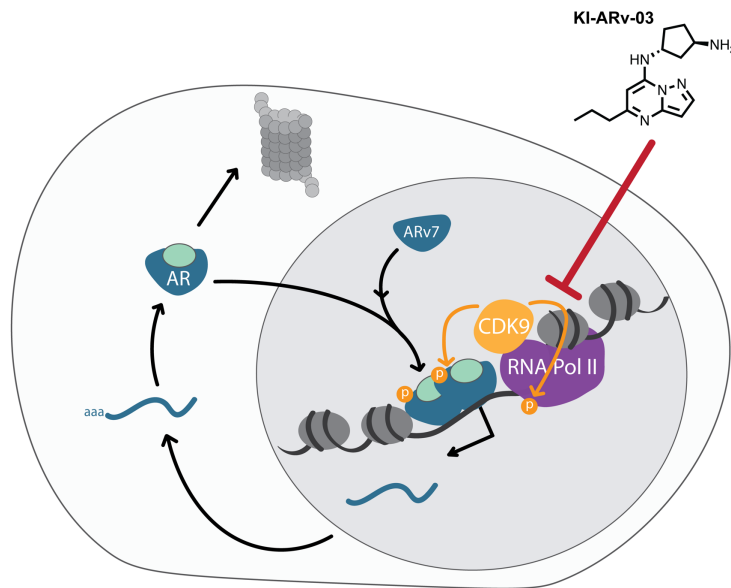


Koryakina, Y., Ta, H. Q., and Gioeli, D. (2014) *Endocr. Relat. Cancer* 21, T131–45

MYC regulates expression of AR and ARVs in PCa

KI-ARv-03 impairs phosphorylation of known CDK9 targets

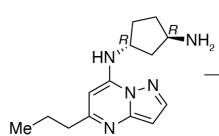
Pol II and AR monitored in 22RV1 cells



Advanced lead KB-0742 shows improved potency while retaining selectivity with activity in preclinical model of prostate cancer

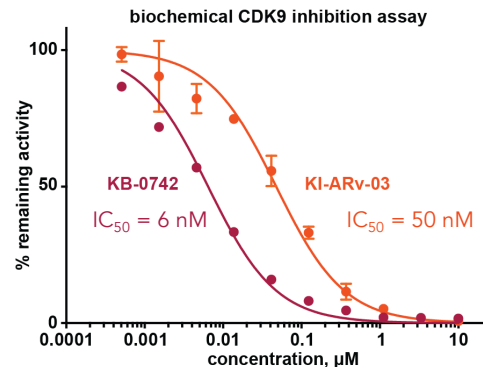
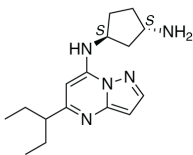
KI-ARv-03

molecular weight: 259.36
cLogP: 1.04



KB-0742

molecular weight: 287.4
cLogP: 1.97

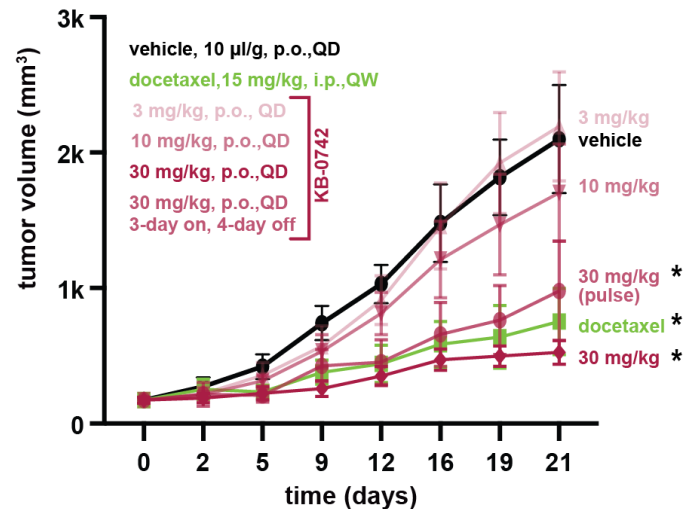


	KB-0742	KI-ARv-03
CDK9	$IC_{50} = 6 \text{ nM}$	$IC_{50} = 50 \text{ nM}$
CDK13	62x	91x
CDK2	66x	200x
CDK12	98x	124x
CDK18	>200x	>200x
CDK3	>200x	>200x
CDK7	>200x	176x
CDK16	>200x	>200x
CDK5	>200x	>200x
CDK17	>200x	>200x
CDK1	>200x	>200x
CDK4	>200x	>200x
CDK6	>200x	>200x
CDK14	>200x	>200x
CDK8	>200x	>200x
CDK19	>200x	>200x

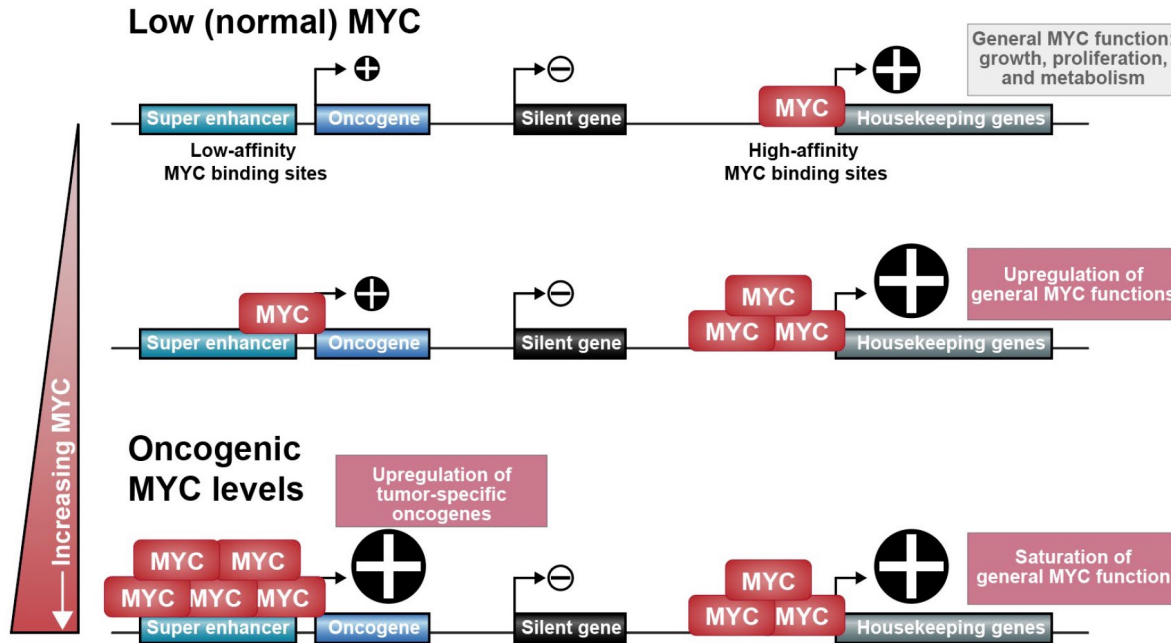
Comparison of relative biochemical IC_{50}

CDK9 fold selectivity vs. $1x$ to $>200x$

tumor outgrowth
22Rv1 xenograft



From L3: Cancers dysregulate MYC by increasing its expression

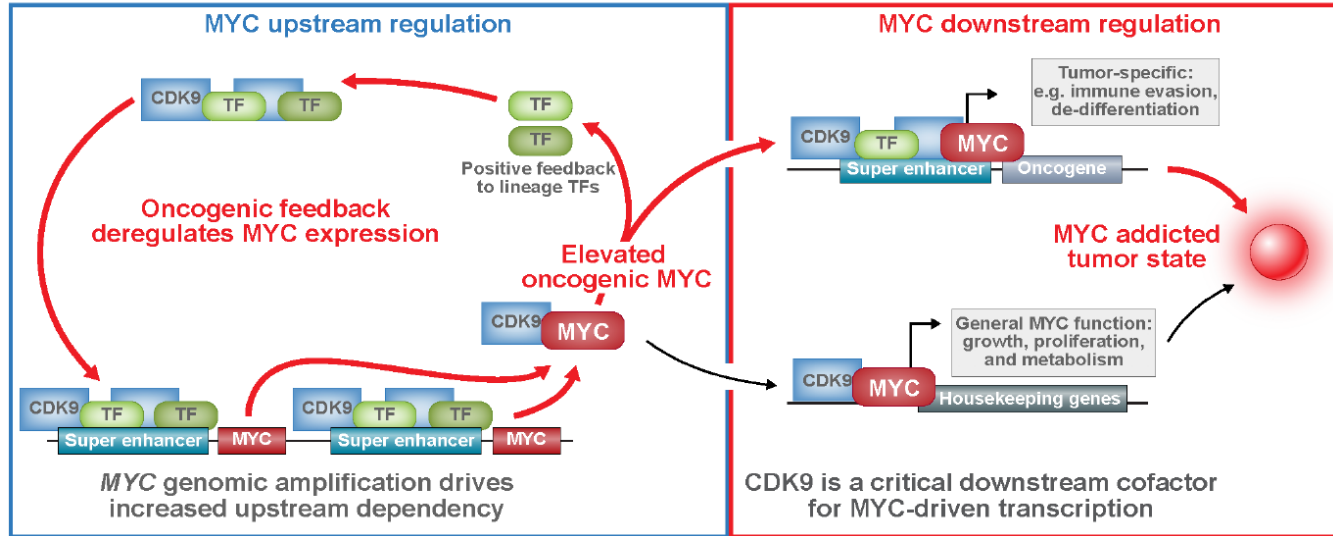


in typical cells, steady state **MYC** levels regulate general housekeeping functions

MYC can be transiently upregulated in typical cells (e.g. during wound healing)

tumor cells need persistently upregulated **MYC** at super physiologic levels to drive tumor-specific oncogenes

Dependence on persistently high MYC expression creates a vulnerability to CDK9 inhibition

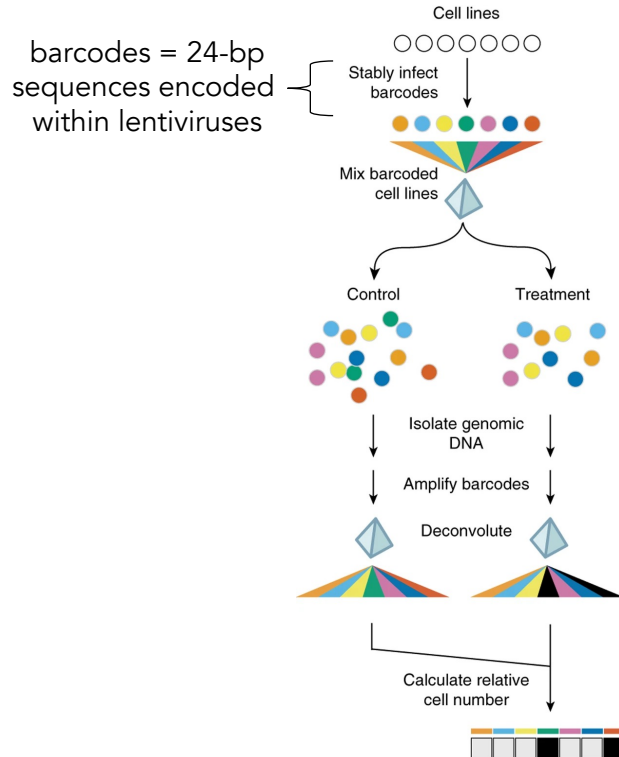


Therapeutic hypothesis:

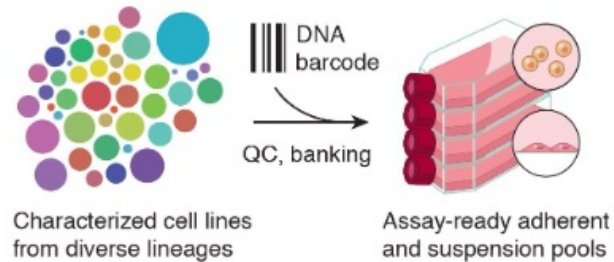
intermittent/partial inhibition of CDK9 may be sufficient to disrupt the oncogenic MYC network

Multiplexed Cell Line Viability Profiling

PRISM is a powerful approach to rapidly screen drugs across hundreds of cancer cell lines



Generation of Barcoded Models for PRISM Screens

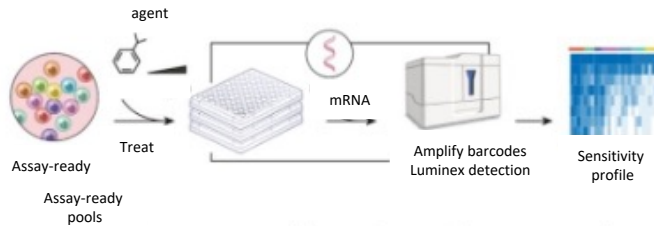


Over 930 genomically characterized CCLE cell lines have been barcoded with a DNA barcode. All cell lines are tested for mycoplasma, verified with SNP fingerprinting, and the barcode identity is confirmed. Cell lines are then mixed together in assay ready pools according to doubling time.

Multiplexed Cell Line Viability Profiling

PRISM is a powerful approach to rapidly screen drugs across hundreds of cancer cell lines

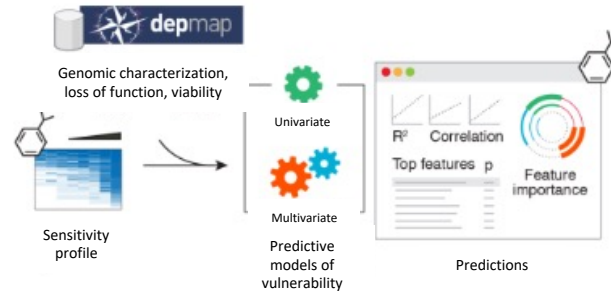
PRISM Viability Assay



Pools of cells are treated for 5 days with compounds, then cells are lysed and mRNA is isolated. The barcode sequences are then amplified by PCR and detected by a Luminex scanner. The quantity of each barcode remaining after treatment serves as a readout to generate cell line sensitivity signatures for each compound.

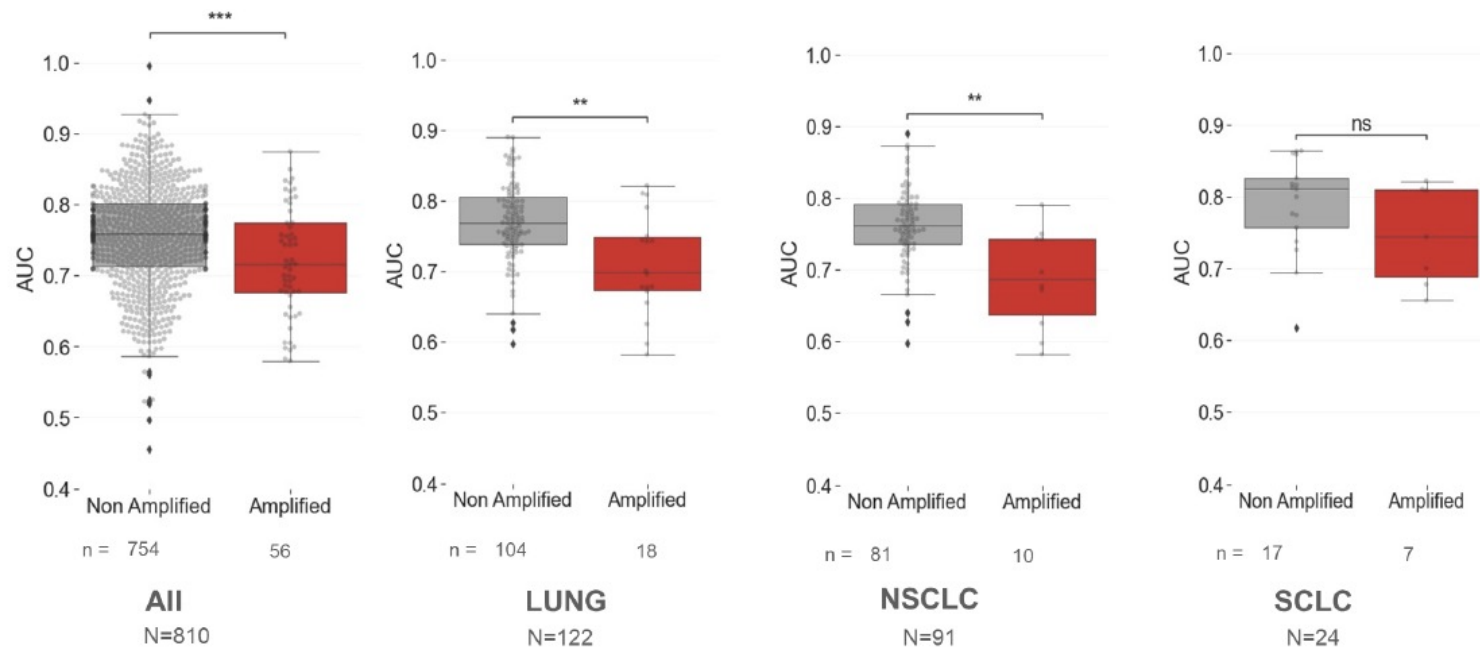
~\$7,000/compound for >900 cell lines

Predictive Modeling



Sensitivity signatures from PRISM data are run through predictive modeling algorithms, such as random forest in order to identify biomarkers using CCLE genomic characterization data, Repurposing drug viability data, and Dependency Map loss-of-function genetic perturbation data.

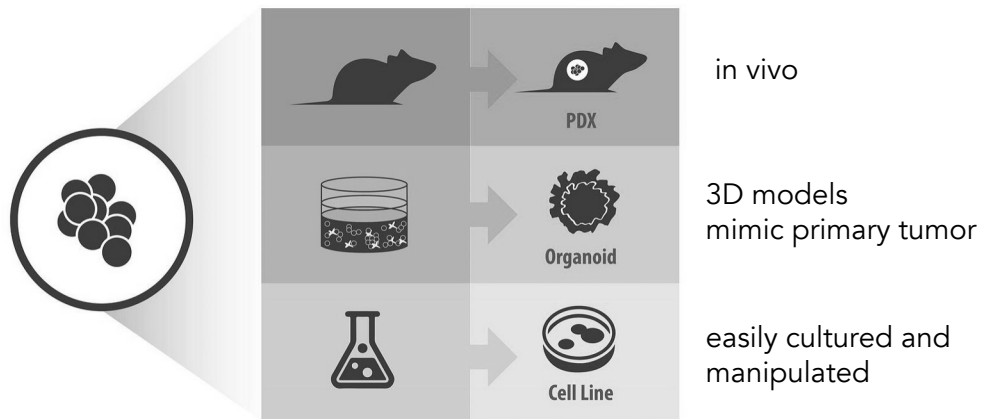
Cancer cell lines with MYC genomic copy number amplification are more sensitive to KB-0742 than non-MYC-amplified lines



Mann-Whitney Wilcoxon test (2-sided with alpha = 0.05)
Amplified = MYC CNA \geq 1.89

KB-0742 is active in patient-derived organoids that express MYC

model types



organoid model description

Model Number	Indication	Treatment history	MYC TPM
KOLU-045	Small Cell Lung Cancer	Naïve	70
KOLU-299		Naïve	30
KOLU-448		Lobaplatin+Etoposide	30
KOLU-775H		Cisplatin	20
KOLU-545H		VP16+Lobaplatin	68
KOLU-643H		VP16 + Lobaplatin	88
KOBR-011	Triple Negative Breast Cancer	TNBC: EPI + PTX 6 cycle	UNK
KOBR-472	TNBC: PTX + CBP 4 cycle	UNK	

KB-0742 is active in patient-derived organoids that express MYC

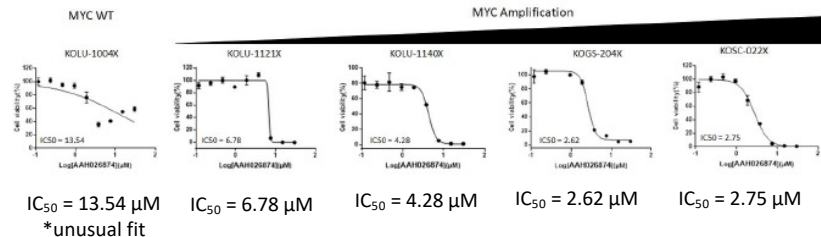
organoid model description

Model Number	Indication	Treatment history	MYC TPM
KOLU-045	Small Cell Lung Cancer	Naïve	70
KOLU-299		Naïve	30
KOLU-448		Lobaplatin+Etoposide	30
KOLU-775H		Cisplatin	20
KOLU-545H		VP16+Lobaplatin	68
KOLU-643H		VP16 + Lobaplatin	88
KOBR-011	Triple Negative Breast Cancer	TNBC: EPI + PTX 6 cycle	UNK
KOBR-472	Triple Negative Breast Cancer	TNBC: PTX + CBP 4 cycle	UNK

drug activity profiles

	Maximum % Inhibition				
	Cisplatin	Pemetrexed	Paclitaxel	Gemcitabine	KB-0742
KOLU-045	10.52	12.83	44.81	53.02	99.99
KOLU-299	10.00	10.00	48.42	57.21	94.19
KOLU-448	10.00	18.97	21.28	34.95	99.02
KOLU-775H	10.00	10.00	49.61	71.74	94.69
KOLU-545H	11.57	4.79	17.50	25.06	95.88
KOLU-643H	No effect	No effect	16.29	No effect	70.65
KOBR-011			31.56	59.99	100.00
KOBR-472	No effect	No effect	No effect	15.06	89.00

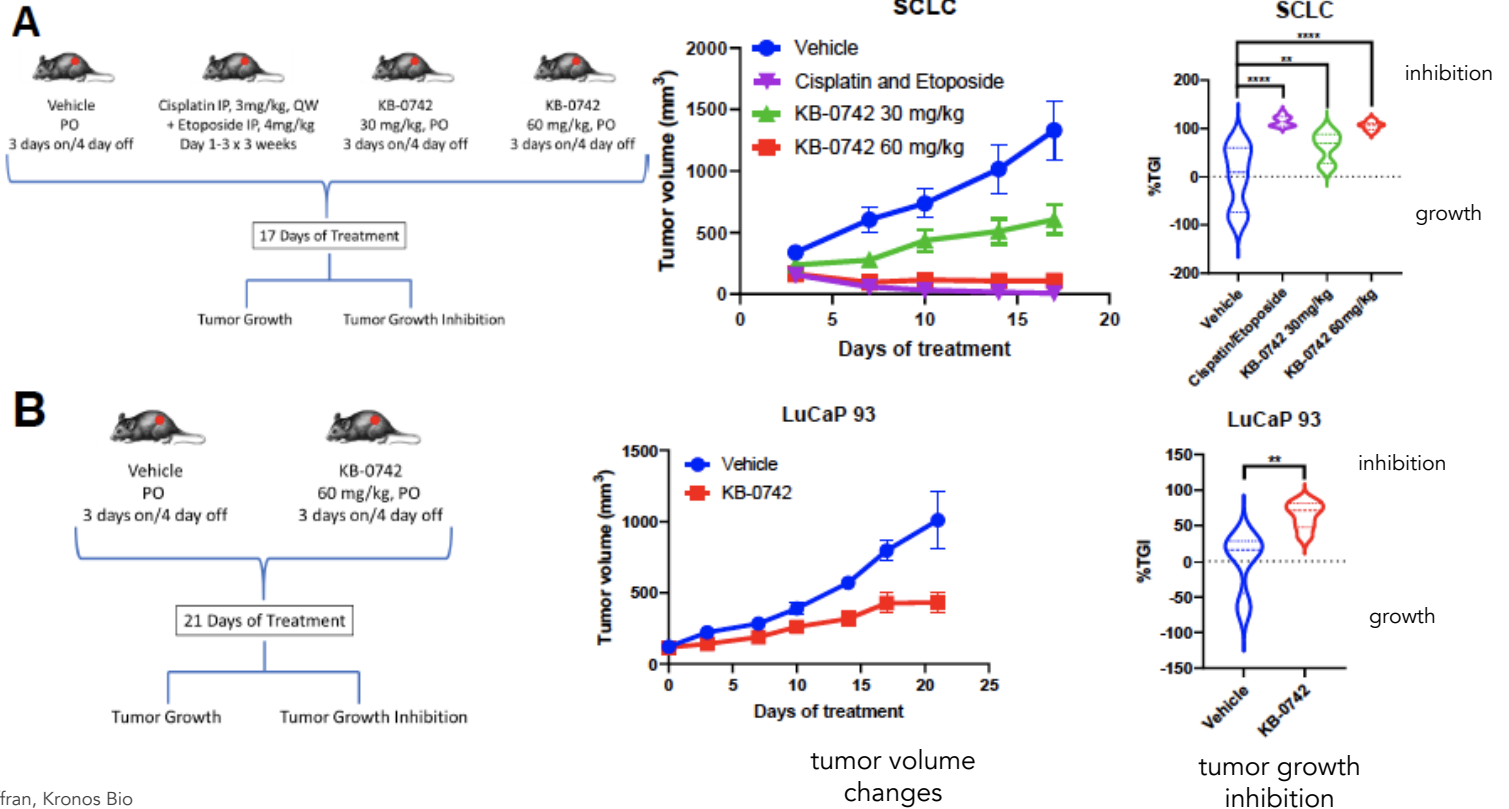
KB-0742 is more potent than standard of care agents (chemo)



KB-0742 shows anti-tumor activity in patient-derived xenografts (PDX)

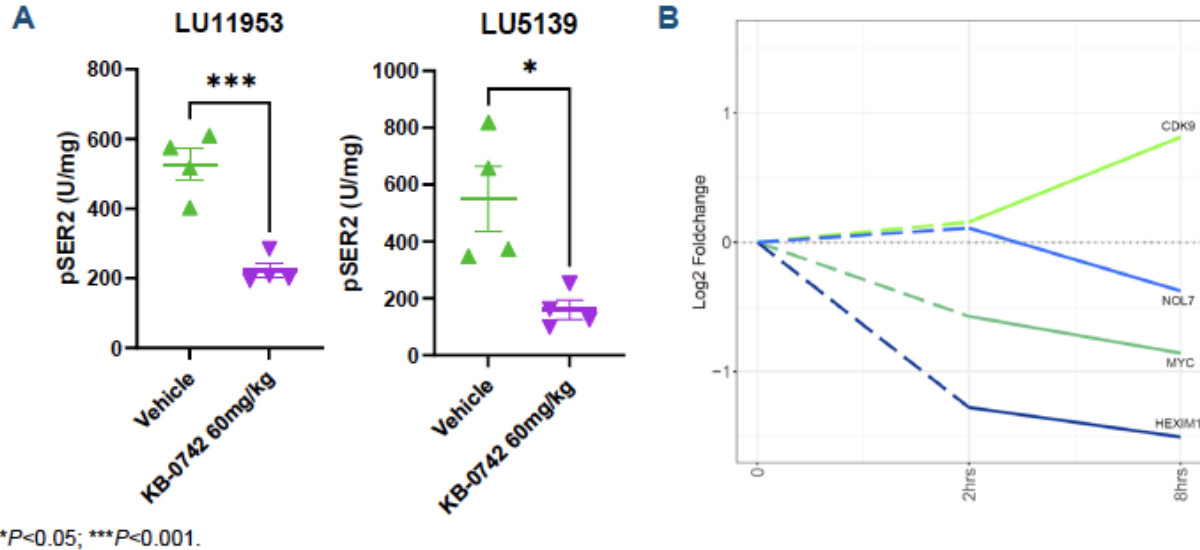
Intermittent dosing in 'MYC high' expressing murine PDX models

subcutaneous
engraftment
of tumor cells
+
treatment



Target engagement in vivo – small cell lung cancer PDX models

KB-0742 reduces phosphorylation of RNA Pol II (pSER2)


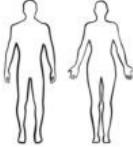
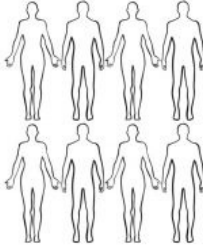

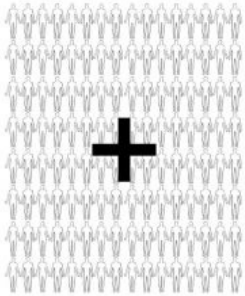


60 mg/kg dose resulted in a 50% or greater reduction in pSer2 after 3 days of dosing

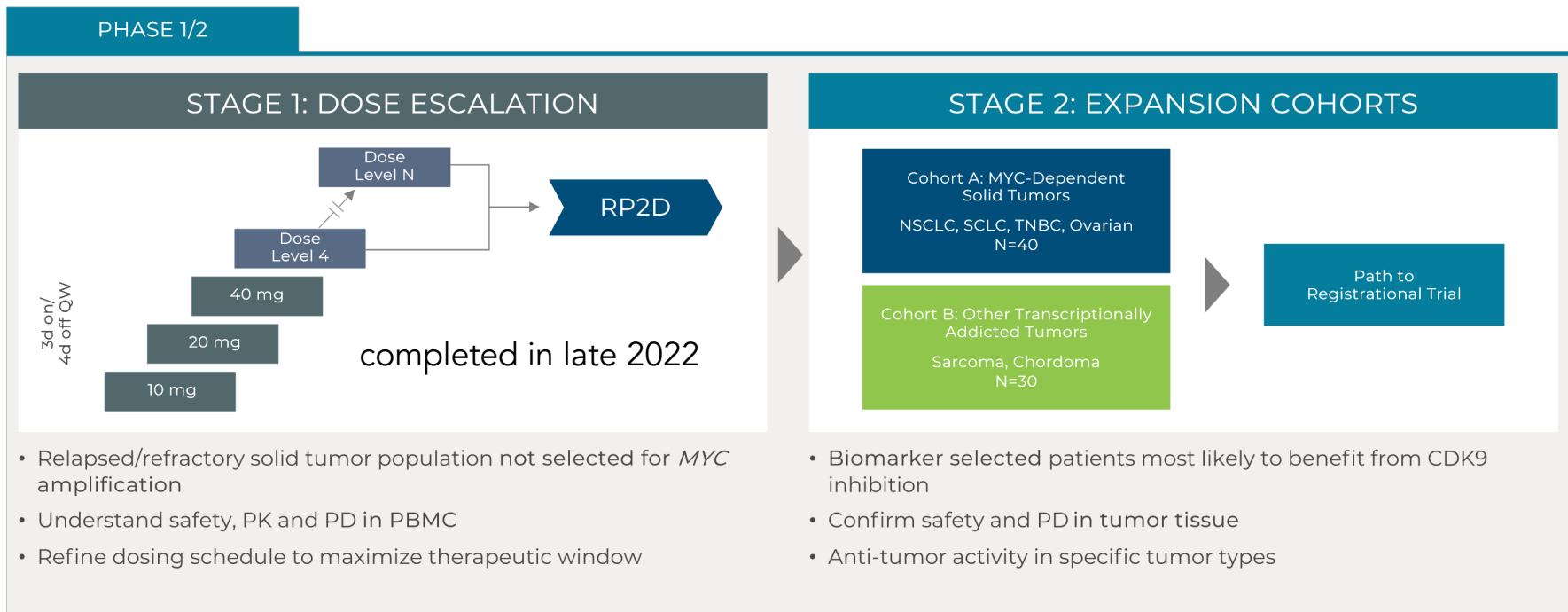
RNA sequencing of LU11953 tumors showed altered gene expression of key genes, including MYC

Clinical Trials

*

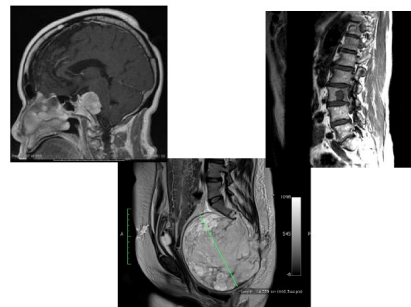
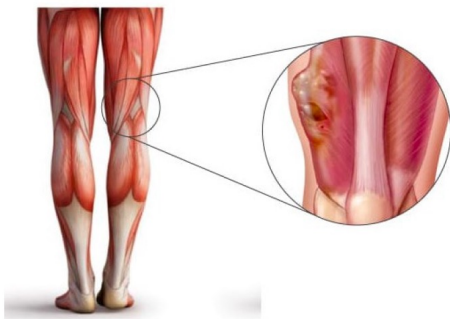
PRECLINICAL	PHASE I	PHASE II	PHASE III	PHASE IV
				
Laboratory Research determines if treatment is useful and safe	6-10 Participants Understand effects of treatment in humans	20-50 Participants Evaluate safety and efficacy of treatment	100-200 Participants Confirm benefit and safety of treatment	200+ Participants Evaluate long-term effects of treatment

KB-0742 Phase 1/2 trial design



RP2D (recommended Phase 2 dose):
60 mg/kg (oral, 3 day on/4 day off) → ~50% reduction in levels of pSer2 on Pol II

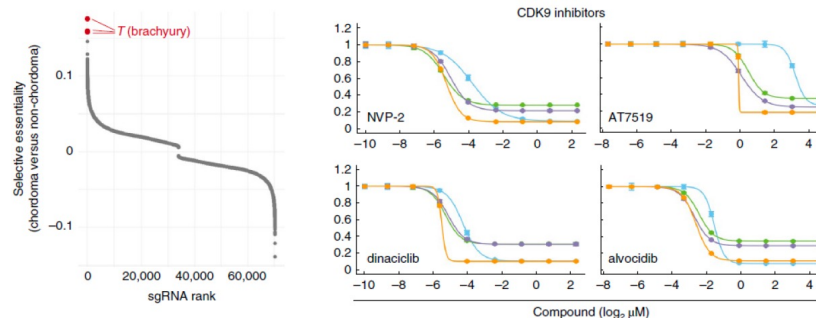
Stage 2 Cohort B will evaluate the anti-tumor activity of KB-0742 in a basket of transcriptionally addicted tumors



Soft-tissue sarcomas with transcription factor fusions as driver mutations, for example:

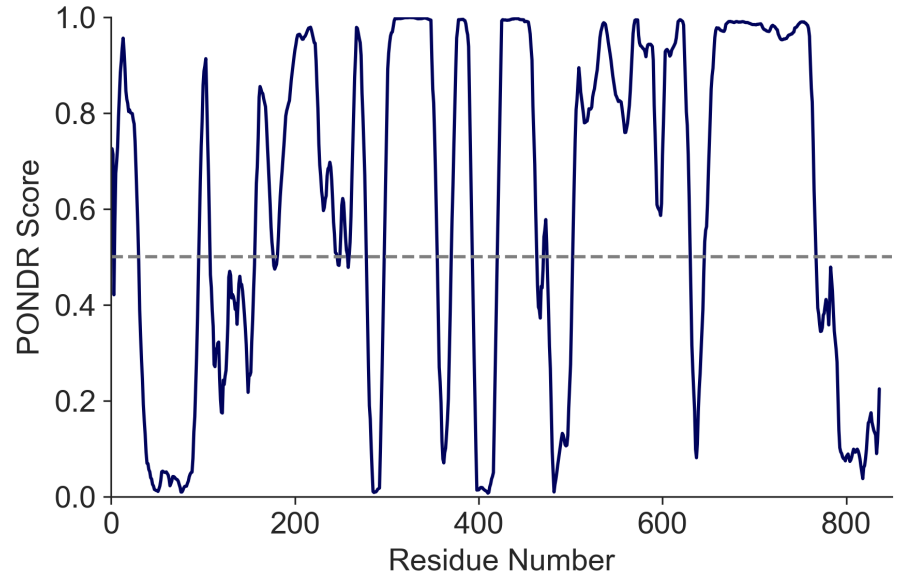
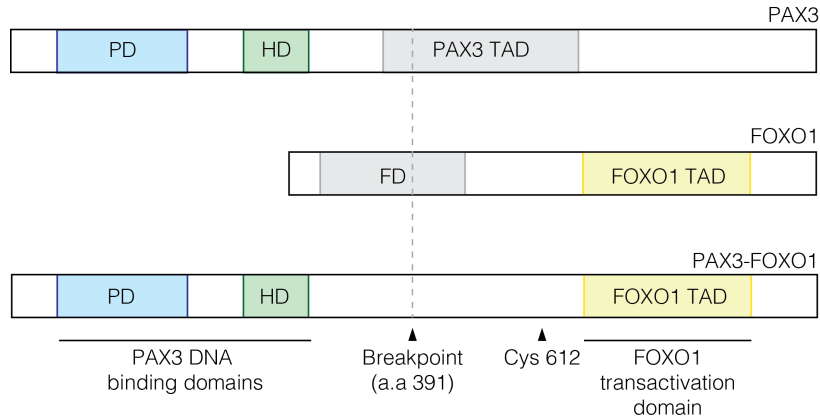
- Ewing sarcoma (EWS-FLI1)
- Rhabdomyosarcoma (PAX-FOXO1)
- Myxoid liposarcoma (FUS-CHOP)
- Clear cell sarcoma (EWSR1-ATF1)
- Desmoplastic round cell tumor (EWSR1-WT1)

Chordoma: dependent on brachyury transcription factor



Sharafinia et al 2019 Nature Med 295:292-300.

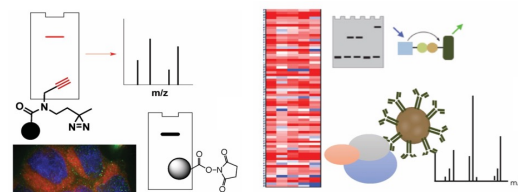
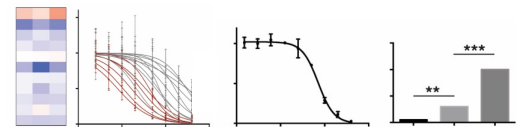
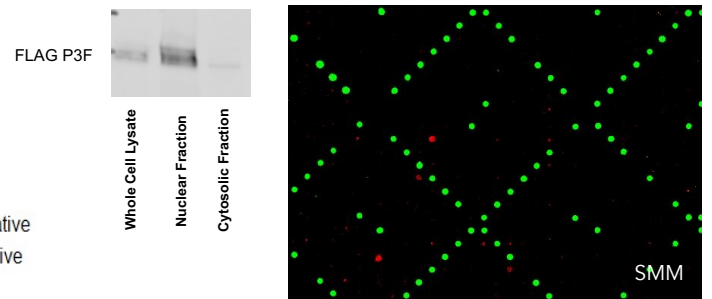
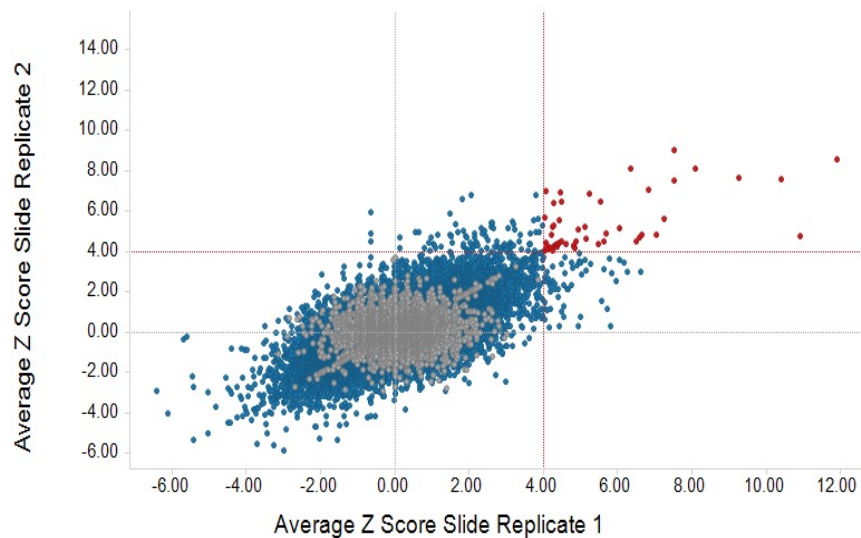
Pathognomonic PAX3-FOXO1 fusion - a highly disordered protein



SMM screens for PAX3-FOXO1

SMM screening data for PAX3-FOXO1 from
Rh4 RMS cell lysates

Screen : ~65,000 small molecules



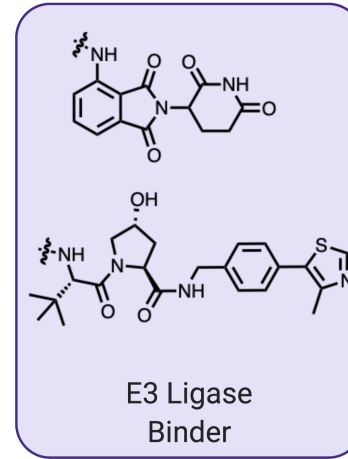
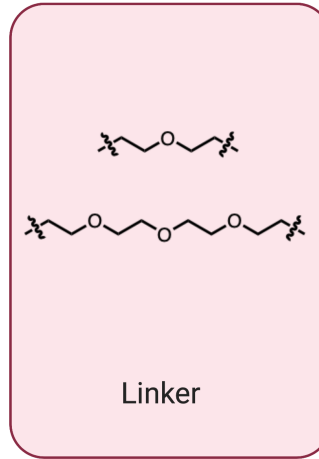
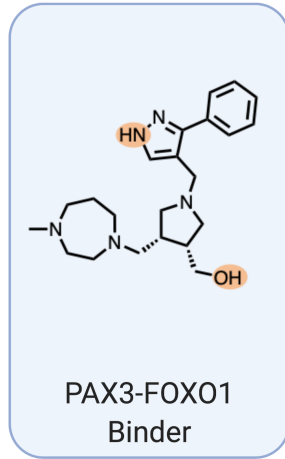
KI-P3F-032 as a starting point for targeted protein degradation (PROTACs)

1. Establish gross SAR

(e.g., CETSA)

2. Establish readouts for P3F degradation

(e.g., HT-western endogenous HiBiT cellular assays)

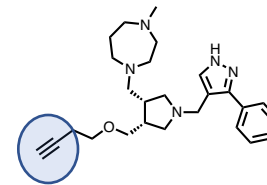
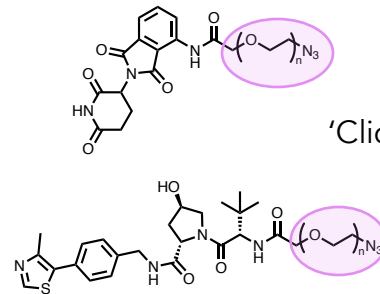
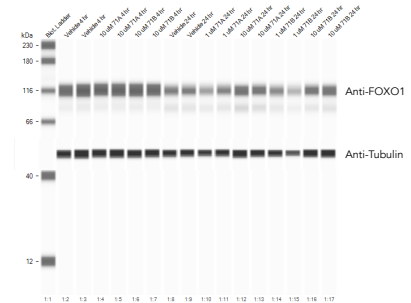


3. Synthesize variants of KI-P3F-032 for coupling

4. Assemble linker library

5. Assembled E3 ligands

6. PROTAC synthesis



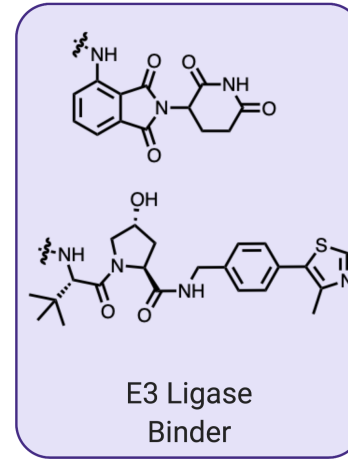
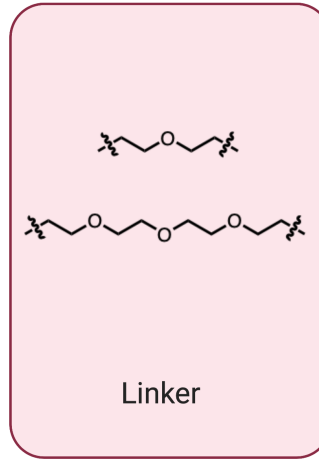
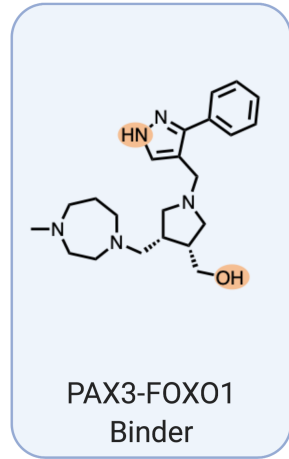
KI-P3F-032 as a starting point for targeted protein degradation (PROTACs)

1. Establish gross SAR

(e.g., CETSA)

2. Establish readouts for P3F degradation

(e.g., HT-western endogenous HiBiT cellular assays)



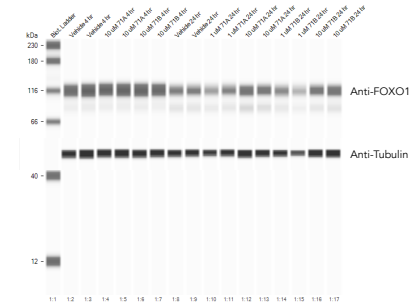
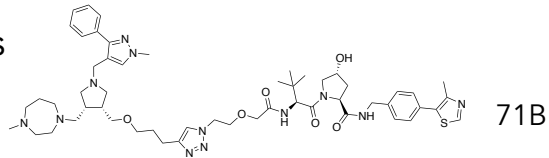
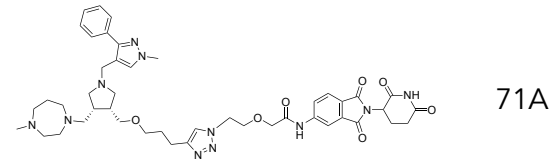
3. Synthesize variants of KI-P3F-032 for coupling

4. Assemble linker library

5. Assembled E3 ligands

6. PROTAC synthesis

PoC degraders candidates for optimization reduce to 80% original P3F levels



Upcoming Lectures

- 2/9/23 Lecture 1 Intro to chemical biology: small molecules, probes, and screens
- 2/14/23 Lecture 2 Small Molecule Microarray (SMM) technique
- 2/16/23 Lecture 3 Our protein target – MAX
- 2/21/23 No Lecture
- 2/23/23 Lecture 4 Quantitative evaluation of protein-ligand interactions
- 2/28/23 Lecture 5 An SMM ligand discovery vignette for sonic hedgehog
- 3/2/23 Lecture 6 KB-0742: A Phase 2 clinical candidate discovered by SMMs
- 3/7/23 Lecture 7 Wrap up discussion for Mod 1 experiments and report